Physics and Applications of Spin Hall Effect

Guang-Yu Guo (郭光宇) [1,2]

[1]**Graduate Institute of Applied Physics,**

National Chengchi University, Taiwan

（政治大學應用物理所）

[2]**Physics Dept, National Taiwan University, Taiwan**

(台灣大學物理系）

(A colloquium in Physics Dept.,

National Tsing Hua Univ., October 20, 2010)

Plan of this Talk

I. Introduction

1. Spin Hall effect.
2. Motivations.

II. Intrinsic spin Hall effect in solids

1. Berry phase formalism for intrinsic Hall effects.
2. Large intrinsic spin Hall effect in platinum

III. Gigantic spin Hall effect in gold and multi-orbital Kondo effect

1. Gigantic spin Hall effect in gold
2. Multi-orbital Kondo effect in Fe impurity in gold.
3. Enhanced SHE by resonant skew scattering in orbital-dependent Kondo effect.
4. Quantum fluctuation in a Kondo system and QMC simulation

IV. Summary and Outlook

1. Topological insulators and quantum spin Hall effect

I. Introduction

1. Spin Hall effect

1) Ordinal Hall Effect

[Hall 1879]

$$\rho_{\mathrm{Hall}} = R_0 B$$

Lorentz force

$q\mathbf{v} \times \mathbf{B}$

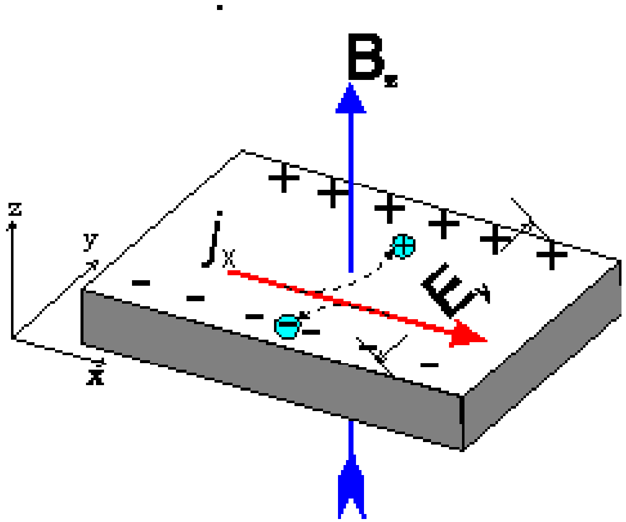

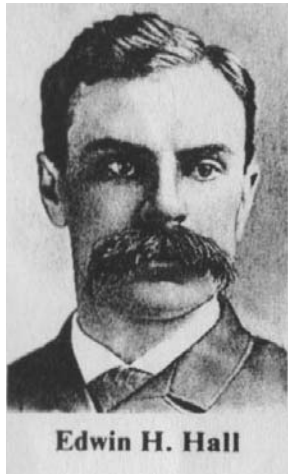

2) Anomalous Hall Effect [Hall, 1880 & 1881]

$$\rho_{\mathrm{Hall}} = R_0 B + R_S M$$

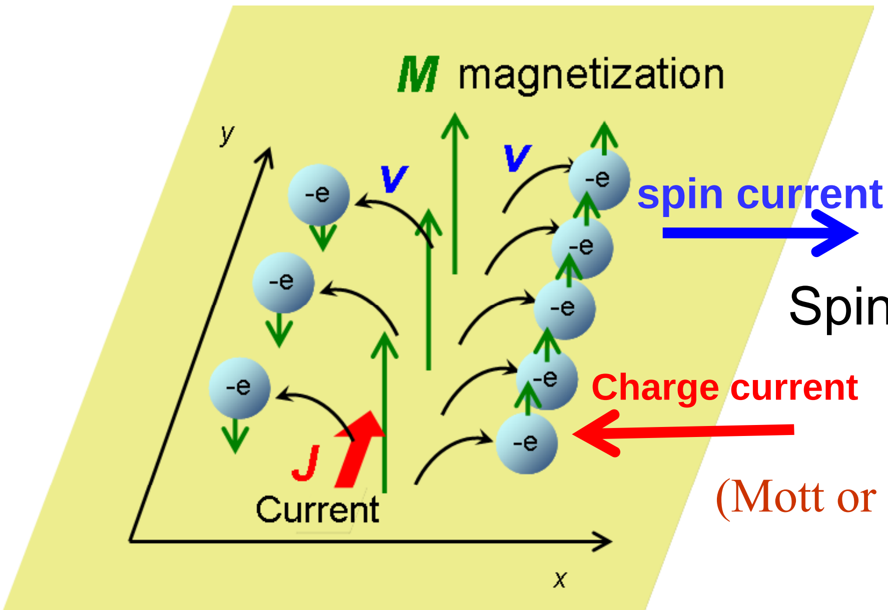

Spin-orbit interaction

$$\frac{dV(r)}{dr}(\mathbf{s} \cdot \mathbf{L})$$

(Mott or skew scattering)

3) (extrinsic) Spin Hall Effect

[Dyakonov & Perel, JETP 1971;
Hirsch, PRL 1999; Zhang, PRL 2000]

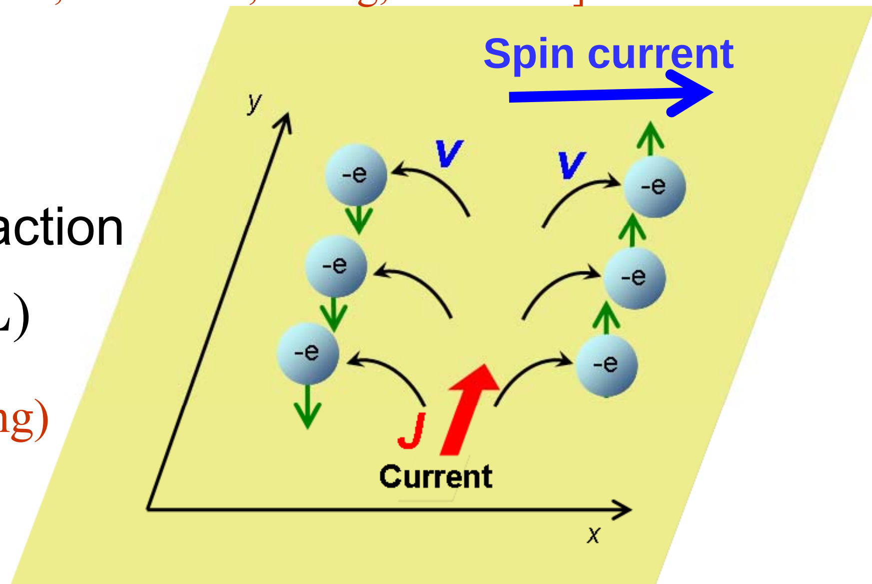

Relativity and spin-orbit interaction

In special relativity, a moving charged particle in an electric field 'feels' a 'magnetic' field [e.g., Jackson's textbook]

$$\vec{B}' = -\gamma \frac{\vec{v}}{c} \times \vec{E} \simeq (\frac{\vec{E} \times \vec{p}}{mc})$$

This 'magnetic' field would then interact with the spin of the particle (electron)

$$H_{SO} = -\vec{\mu} \cdot \vec{B}' = \frac{(g-1)e}{2mc} \vec{s} \cdot (\frac{\vec{E} \times \vec{p}}{mc^2}) \simeq -\frac{1}{2m^2c^2} \vec{s} \cdot (\nabla V(\mathbf{r}) \times \vec{p})$$

For a spherical symmetric atomic potential (e.g., near the nucleus),

$$H_{SO} = -\frac{1}{2m^2c^2} \vec{s} \cdot (\frac{dV}{dr} \frac{\vec{r}}{r} \times \vec{p}) = -\frac{1}{2m^2c^2 r} \frac{dV}{dr} (\vec{s} \cdot \vec{L}) \approx -\frac{Ze^2}{2m^2c^2r^3} (\vec{s} \cdot \vec{L})$$

4) Intrinsic spin Hall effect

(1) In p-type zincblende semiconductors

Dissipationless Quantum Spin Current at Room Temperature

Shuichi Murakami,[1*] Naoto Nagaosa,[1,2,3] Shou-Cheng Zhang[4]

5 SEPTEMBER 2003 VOL 301 SCIENCE www.sciencemag.org

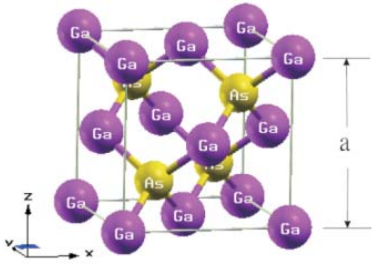

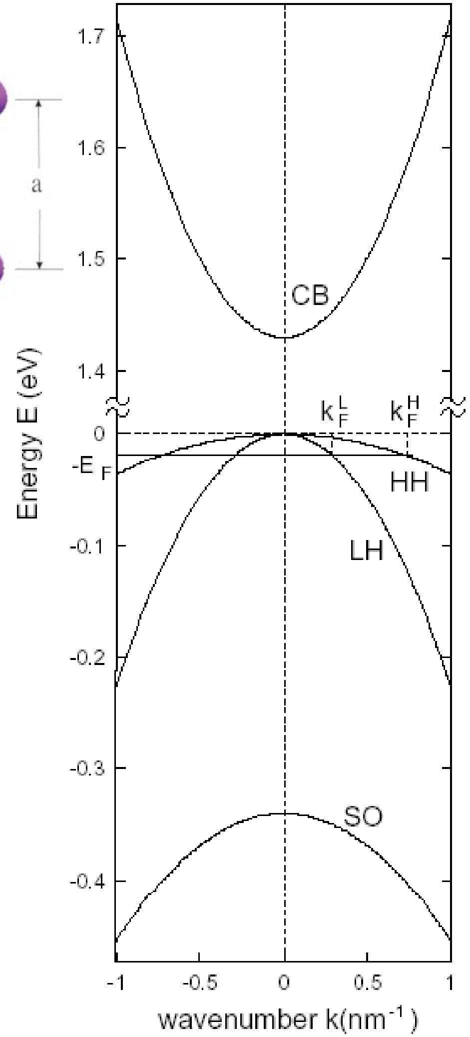

Luttinger model $$H_0 = \frac{\hbar^2}{2m}\left[(\gamma_1 + \frac{5}{2}\gamma_2)k^2 - 2\gamma_2(\vec{k}\cdot\vec{S})^2\right]$$

Equation of motion $$\left\langle \dot{X}_i \right\rangle = \frac{\hbar k_i}{m_\lambda} + F_{il}\left\langle \dot{k}_l \right\rangle$$

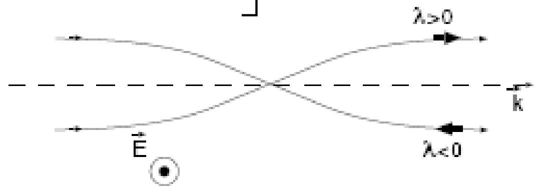

$$\left\langle \dot{k}_i \right\rangle = \frac{e}{\hbar}E_i \qquad e > 0 \text{ (hole)}$$

Anomalous velocity $$\left\langle \dot{\vec{X}} \right\rangle = \frac{\hbar\vec{k}}{m_\lambda} - \frac{e\lambda}{\hbar k^3}\vec{k}\times\vec{E}$$

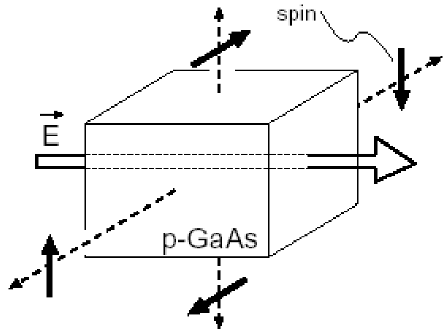

$$j_j^i = \sigma_s \varepsilon^{ijk} E_k \qquad (1)$$

$$j_y^x = \frac{eE_z}{12\pi^2}(3k_F^{\mathrm{H}} - k_F^{\mathrm{L}}) = \frac{\hbar}{2e}\sigma_s E_z \quad (10)$$

$n_h = 10^{19}\ \mathrm{cm}^{-3}$, $\mu = 50$ cm /V·s, $\sigma = e\mu n_h = 80\ \Omega^{-1}\mathrm{cm}^{-1}$; $\sigma_s = 80\ \Omega^{-1}\mathrm{cm}^{-1}$

$n_h = 10^{16}\ \mathrm{cm}^{-3}$, $\mu = 50$ cm /V·s, $\sigma = e\mu n_h = 0.6\ \Omega^{-1}\mathrm{cm}^{-1}$; $\sigma_s = 7\ \Omega^{-1}\mathrm{cm}^{-1}$

(2) In a 2-D electron gas in n-type semiconductor heterostructures

Universal Intrinsic Spin Hall Effect

Jairo Sinova,[1,2] Dimitrie Culcer,[2] Q. Niu,[2] N. A. Sinitsyn,[1] T. Jungwirth,[2,3] and A. H. MacDonald[2]
[1]Department of Physics, Texas A&M University, College Station, Texas 77843-4242, USA
[2]Department of Physics, University of Texas at Austin, Austin, Texas 78712-1081, USA
[3]Institute of Physics ASCR, Cukrovarnická 10, 162 53 Praha 6, Czech Republic
(Received 27 July 2003; published 25 March 2004)

Rashba Hamiltonian

$$H = \frac{p^2}{2m} - \frac{\lambda}{\hbar}\vec{\sigma}\cdot(\hat{z}\times\vec{p}), \quad (1)$$

contributes to the spin current. In this case we find that the spin current in the $\hat{y}$ direction is [23]

$$j_{s,y} = \int_{\text{annulus}} \frac{d^2\vec{p}}{(2\pi\hbar)^2}\frac{\hbar n_{z,\vec{p}}}{2}\frac{p_y}{m} = \frac{-eE_x}{16\pi\lambda m}(p_{F+} - p_{F-}), \quad (6)$$

where p_{F+} and p_{F-} are the Fermi momenta of the majority and minority spin Rashba bands. We find that when both bands are occupied, i.e., when $n_{2D} > m^2\lambda^2/\pi\hbar^4 \equiv n^*_{2D}$, $p_{F+} - p_{F-} = 2m\lambda/\hbar$ and then the spin Hall (sH) conductivity is

Universal spin Hall conductivity

$$\sigma_{sH} \equiv -\frac{j_{s,y}}{E_x} = \frac{e}{8\pi}, \quad (7)$$

independent of both the Rashba coupling strength and of the 2DES density. For $n_{2D} < n^*_{2D}$ the upper Rashba band is depopulated. In this limit p_{F-} and p_{F+} are the interior and exterior Fermi radii of the lowest Rashba split band, and σ_{sH} vanishes linearly with the 2DES density:

$$\sigma_{sH} = \frac{e}{8\pi}\frac{n_{2D}}{n^*_{2D}}. \quad (8)$$

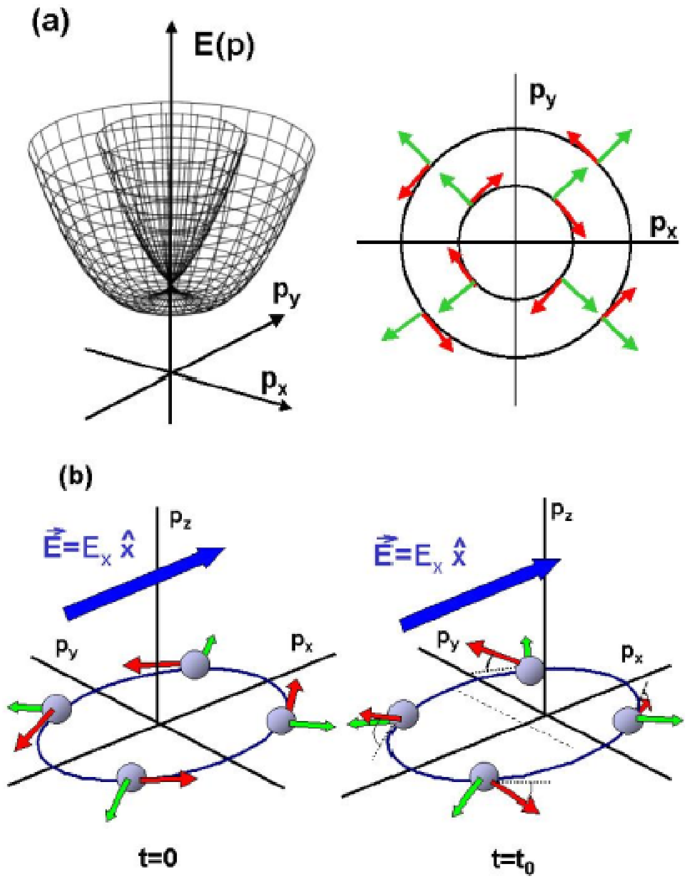

(3) Significances of these theoretical discoveries of intrinsic spin Hall effects

Basic elements of spintronics (spin electronics):

Generation, detection, & manipulation of spin current.

Usual spin current generations:

Ferromagnetic leads

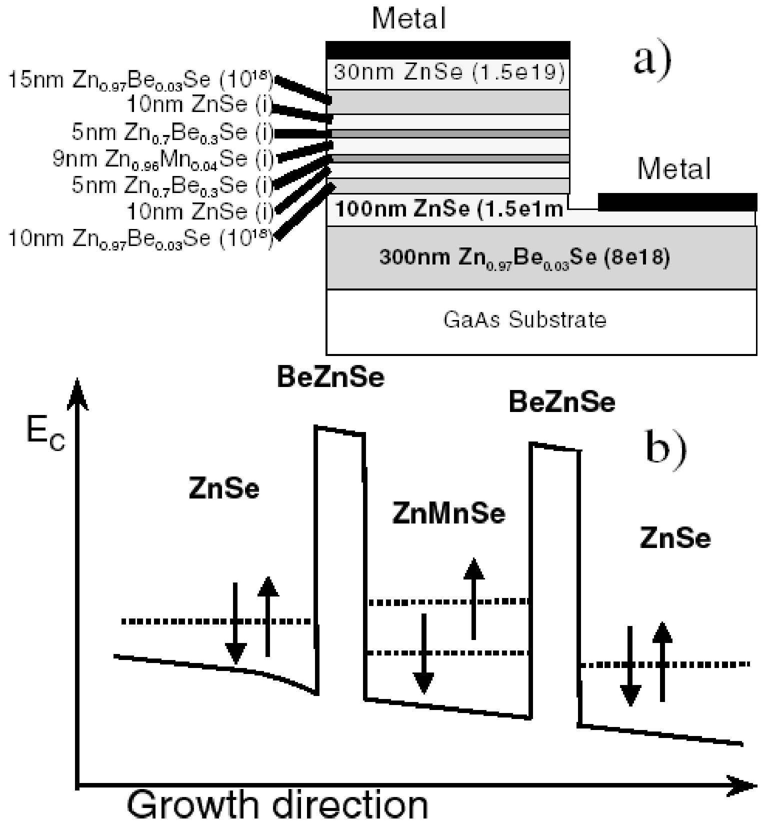

FIG. 1. (a) Layer structure of the device and (b) schematic view of resonant tunnel diode band structure under bias.

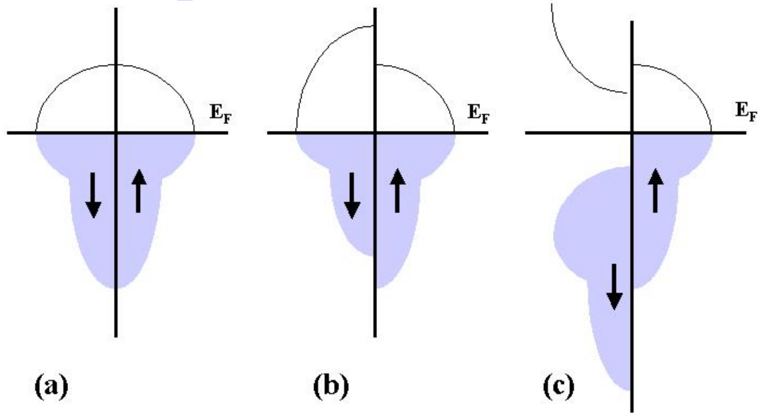

(a) non-magnetic metals, (b) ferromagnetic metals and (c) half-metallic metals.

Spin filter [Slobodskyy, et al., PRL 2003]

Problems: magnets and/or magnetic fields needed, and difficult to integrate with semiconductor technologies.

Among other things,
it would enable us to generate spin current electrically in semiconductor microstructures without applied magnetic fields or magnetic materials,
and hence make possible pure electric driven spintronics in semiconductors which could be readily integated with conventional electronics.

5) Experiments on spin Hall effect

(a) in n-type 3D GaAs and InGaAs thin films

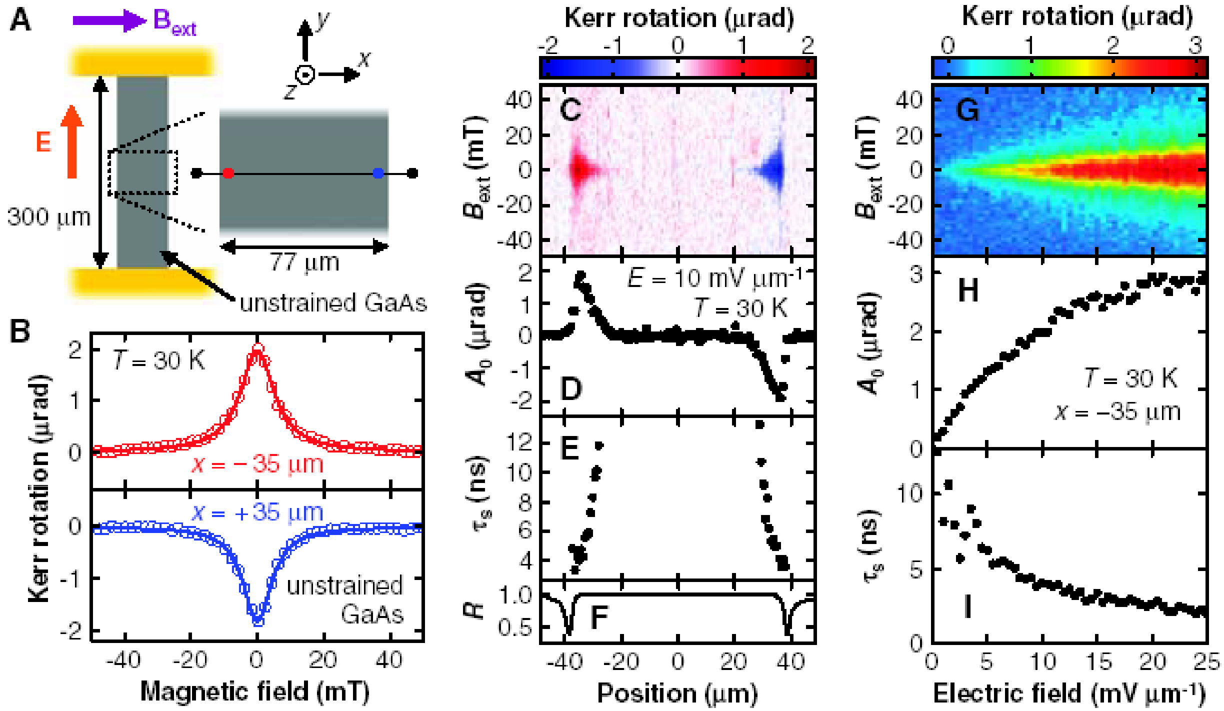

Fig. 1. The spin Hall effect in unstrained GaAs. Data are taken at $T = 30$ K; a linear background has been subtracted from each B_{ext} scan. (**A**) Schematic of the unstrained GaAs sample and the experimental geometry. (**B**) Typical measurement of KR as a function of B_{ext} for $x = -35$ μm (red circles) and $x = +35$ μm (blue circles) for $E = 10$ mV μm^{-1}. Solid lines are fits as explained in text. (**C**) KR as a function of x and B_{ext} for $E = 10$ mV μm^{-1}. (**D** and **E**) Spatial dependence of peak KR A_0 and spin lifetime τ_s across the channel, respectively, obtained from fits to data in (C). (**F**) Reflectivity R as a function of x. R is normalized to the value on the GaAs channel. The two dips indicate the position of the edges and the width of the dips gives an approximate spatial resolution. (**G**) KR as a function of E and B_{ext} at $x = -35$ μm. (**H** and **I**) E dependence of A_0 and τ_s, respectively, obtained from fits to data in (G).

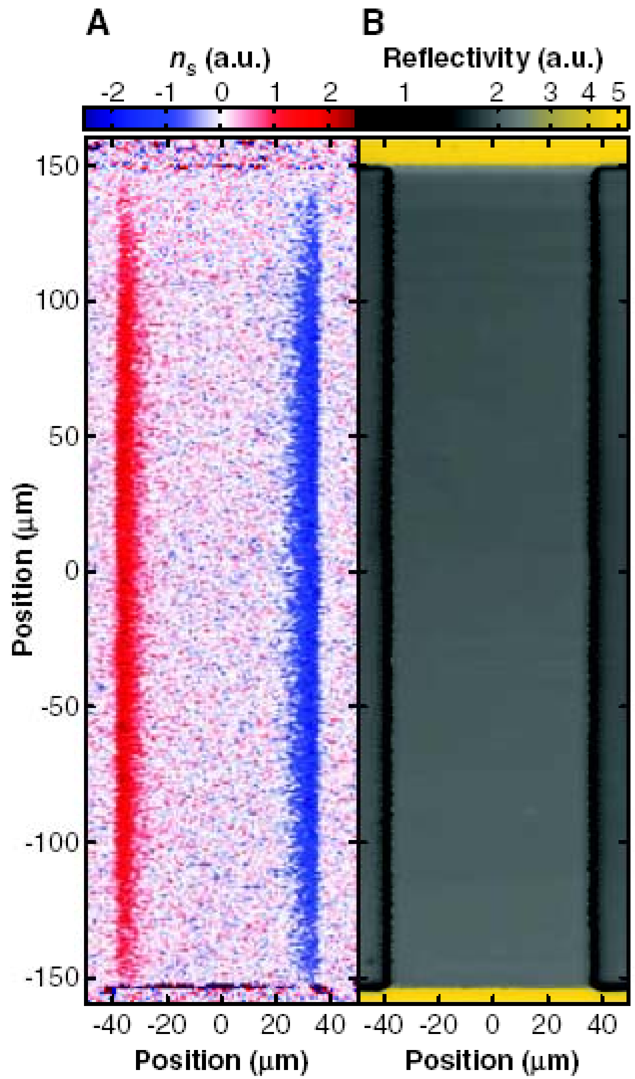

Fig. 2. (**A** and **B**) Two-dimensional images of spin density n_s and reflectivity R, respectively, for the unstrained GaAs sample measured at $T = 30$ K and $E = 10$ mV μm^{-1}.

[Kato *et al.*, Science 306, 1910 (2004)]

Attributed to extrinsic SHE because of weak crystal direction dependence.

(b) in p-type 2D semiconductor quantum wells

Experimental Observation of the Spin-Hall Effect in a Two-Dimensional Spin-Orbit Coupled Semiconductor System

J. Wunderlich,[1] B. Kaestner,[1,2] J. Sinova,[3] and T. Jungwirth[4,5]

[1]*Hitachi Cambridge Laboratory, Cambridge CB3 0HE, United Kingdom*
[2]*National Physical Laboratory, Teddington T11 0LW, United Kingdom*
[3]*Department of Physics, Texas A&M University, College Station, Texas 77843-4242, USA*
[4]*Institute of Physics ASCR, Cukrovarnická 10, 162 53 Praha 6, Czech Republic*
[5]*School of Physics and Astronomy, University of Nottingham, Nottingham NG7 2RD, United Kingdom*

(Received 16 November 2004; published 4 February 2005)

We report the experimental observation of the spin-Hall effect in a 2D hole system with spin-orbit coupling. The 2D hole layer is a part of a *p-n* junction light-emitting diode with a specially designed coplanar geometry which allows an angle-resolved polarization detection at opposite edges of the 2D hole system. In equilibrium the angular momenta of the spin-orbit split heavy-hole states lie in the plane of the 2D layer. When an electric field is applied across the hole channel, a nonzero out-of-plane component of the angular momentum is detected whose sign depends on the sign of the electric field and is opposite for the two edges. Microscopic quantum transport calculations show only a weak effect of disorder, suggesting that the clean limit spin-Hall conductance description (intrinsic spin-Hall effect) might apply to our system.

DOI: 10.1103/PhysRevLett.94.047204 PACS numbers: 75.50.Pp, 71.70.Ej, 85.75.Mm

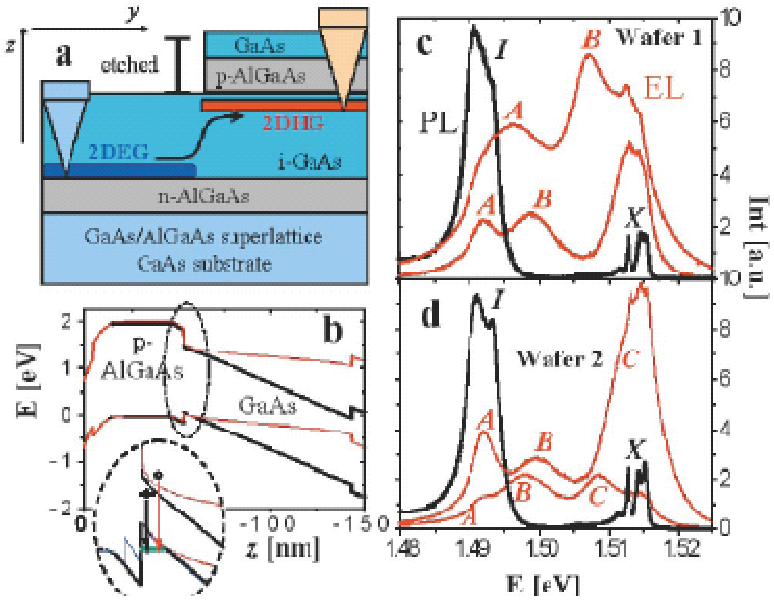

[Wunderlich, et al., PRL 94 (2005) 047204]

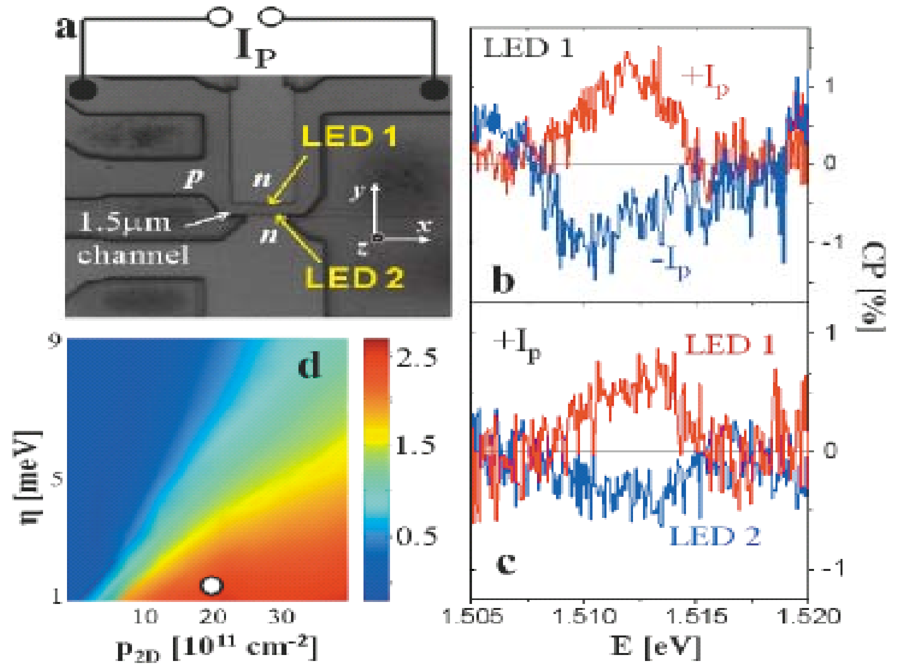

Attributed to intrinsic SHE.

(c) Spin Hall effect in strained *n*-type wurtzite semiconductors

[Chang, Chen, Chen, Hong, Tsai, Chen, Guo, PRL 98, 136403 (2007)]

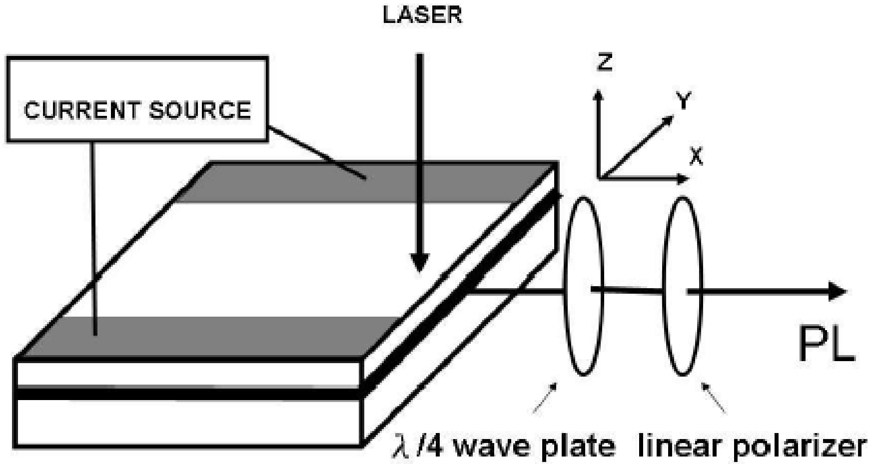

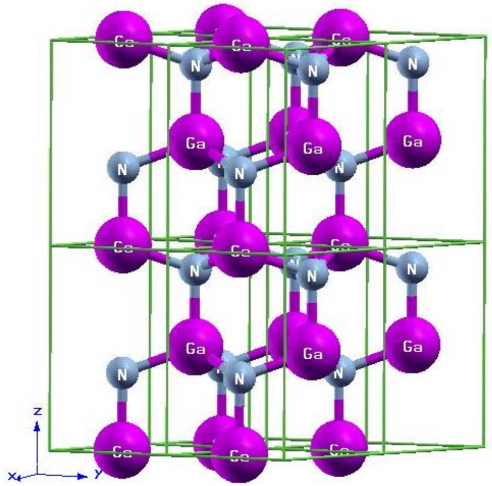

n-type (5nm $In_xGa_{1-x}N$/3nm GaN) superlattice (x=0.15)

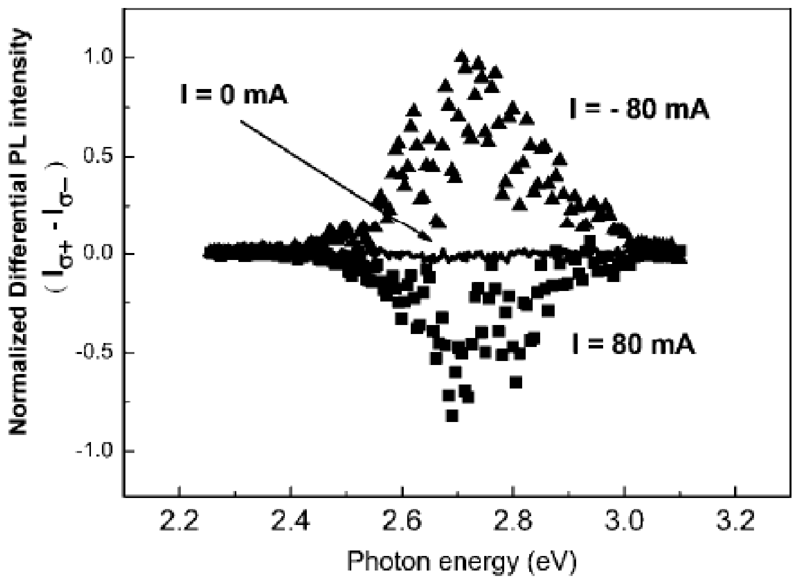

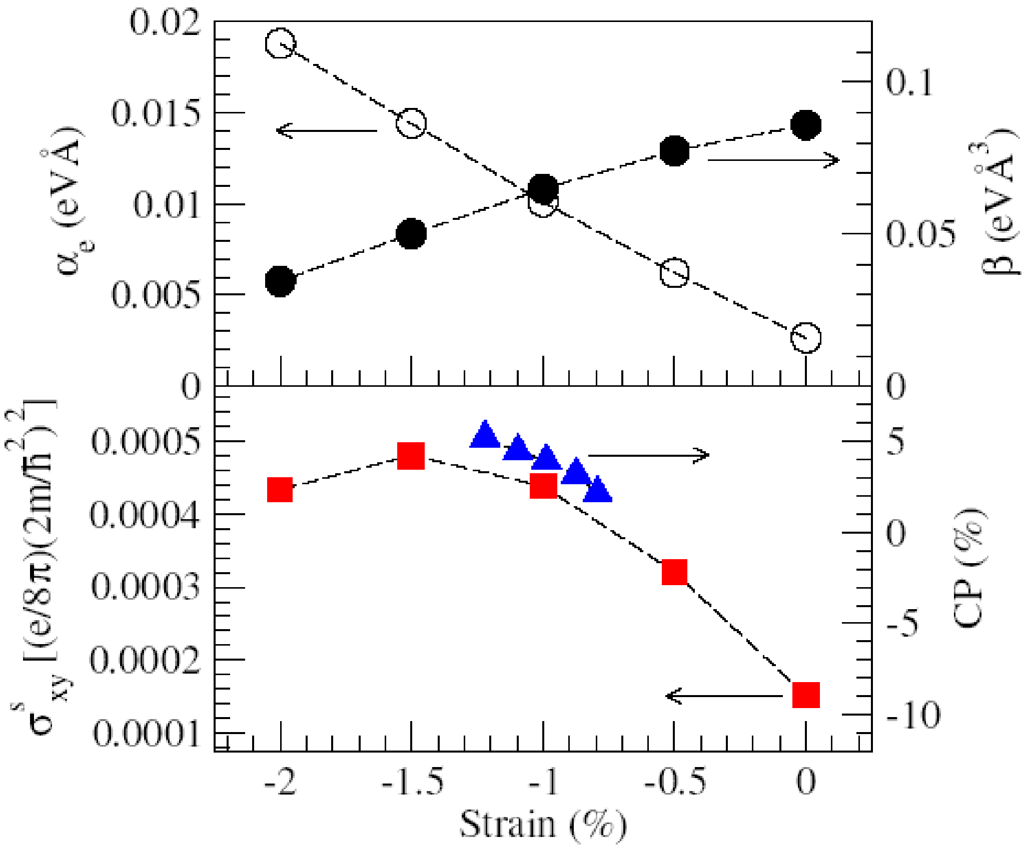

2. Motivations

1) Questions on the intrinsic spin Hall effect in semiconductors?

[in the summer of 2004]

(1) Non-existence of intrinsic spin Hall effect in bulk *p*-type semiconductor? [X. Wang and X.-G. Zhang, cond-mat/0407699; JMMM 2005]

In conclusion, we have shown that at least for a class of semiconductors described by the Luttinger Hamiltonian, spin symmetry of the eigenstates rules out the possibility of a spontaneous spin current in these materials.

(2) Will the intrinsic spin Hall effect exactly cancelled by the intrinsic orbital-angular-momentum Hall effect? [S. Zhang and Z. Yang, cond-mat/0407704; PRL 2005]

In conclusion, we have shown that the ISHE is accompanied by the intrinsic orbital-angular-momentum Hall effect so that the total angular momenttum spin current is zero in a SOC system.

For Rashba Hamiltonian, $\mathcal{J}_{int}^{spin} = \frac{e}{8\pi}E; \quad J_{int}^{orbit} = -\frac{e}{8\pi}E.$

This is confirmed for Rashba system by us. However, in Dresselhaus and Rashba systems, spin Hall conductivity would not be cancelled by the orbital Hall conductivity.

[Chen, Huang, Guo, PRB73 (2006) 235309]

Motivations

(1) Try to resolve the above two important problems.

(2) To go beyond the spherical 4-band Luttinger Hamiltonian.

(3) To understand the effects of epitaxial strains.

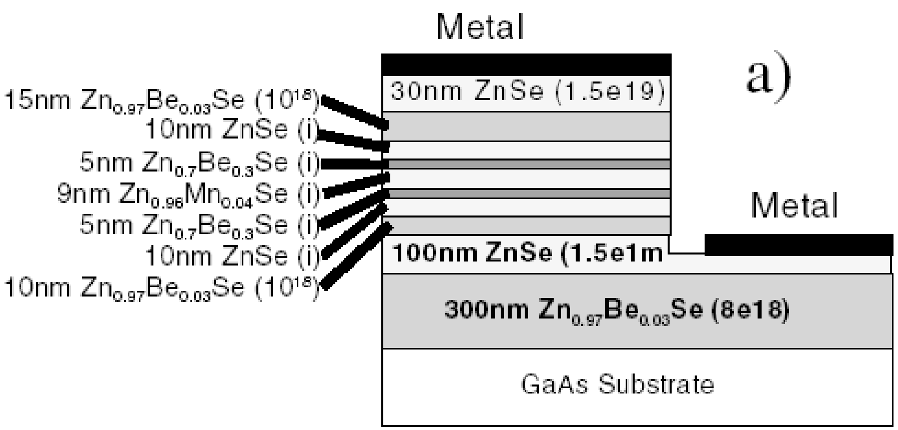

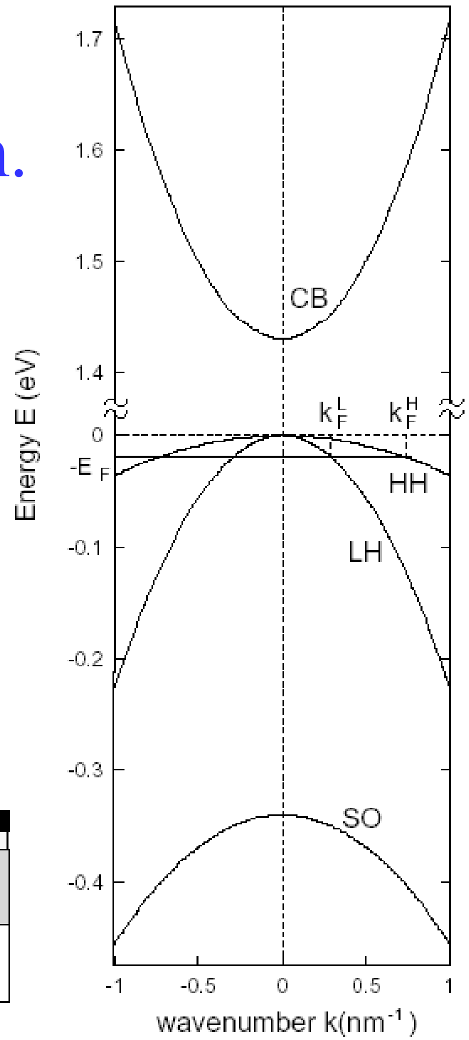

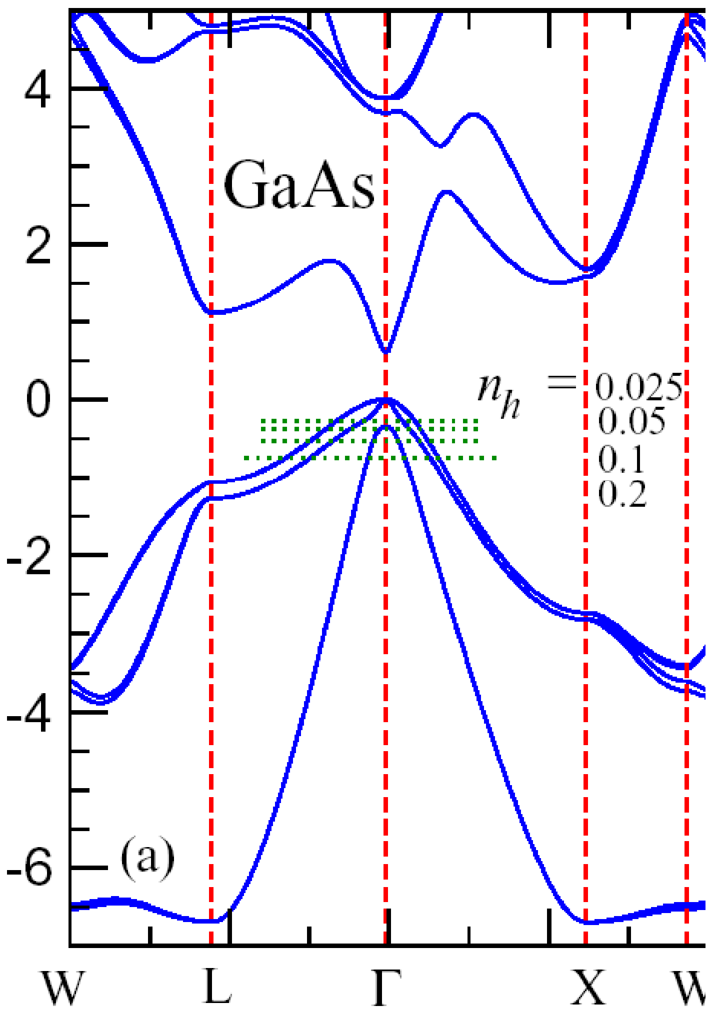

2) Spin Hall effect in metals

Nature 13 July 2006 Vol. 442, P. 04937

Direct electronic measurement of the spin Hall effect

S. O. Valenzuela[1]† & M. Tinkham[1]

fcc Al

$\sigma_{sH} = 27\sim34\ (\Omega\mathrm{cm})^{-1}$
(T= 4.2 K)

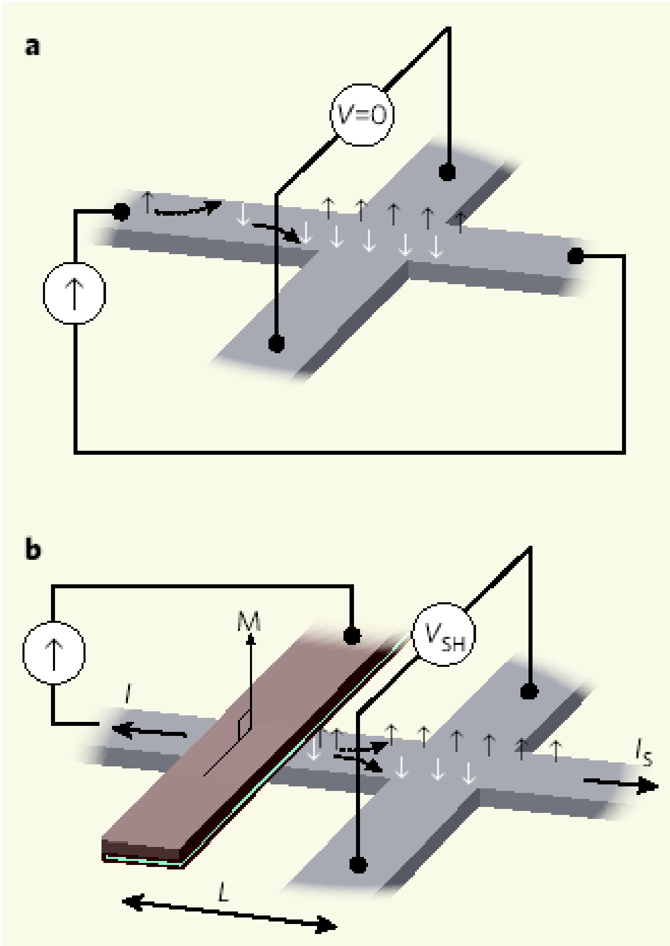

Room Temperature Reversible Spin Hall Effect

[PRL98, 156601; 98 (2007), 139901 (E) (2007)]

T. Kimura,[1,2] Y. Otani,[1,2] T. Sato,[1] S. Takahashi,[3,4] and S. Maekawa[3,4]

[1] Institute for Solid State Physics, University of Tokyo

$\sigma_{sH} = 240\ (\Omega\mathrm{cm})^{-1}$
(T= 290 K)

Assumed to be extrinsic!

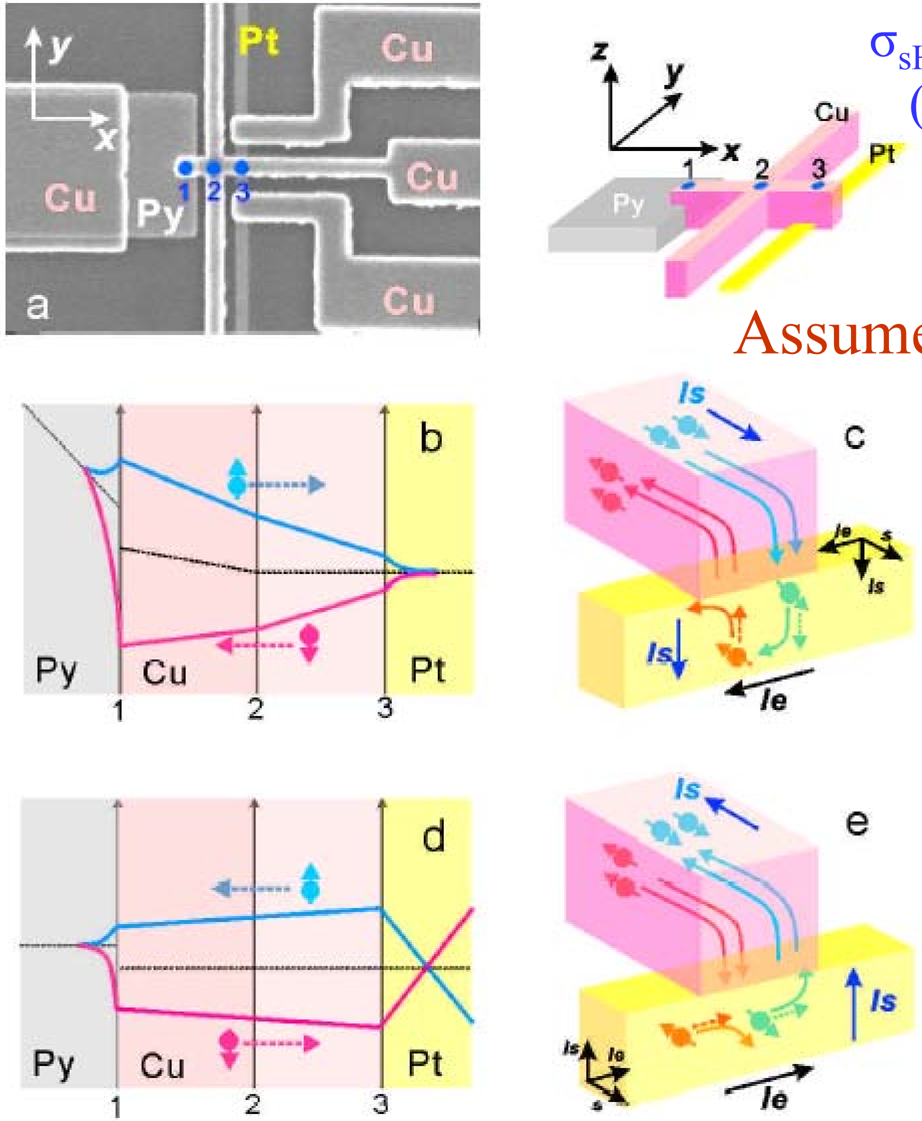

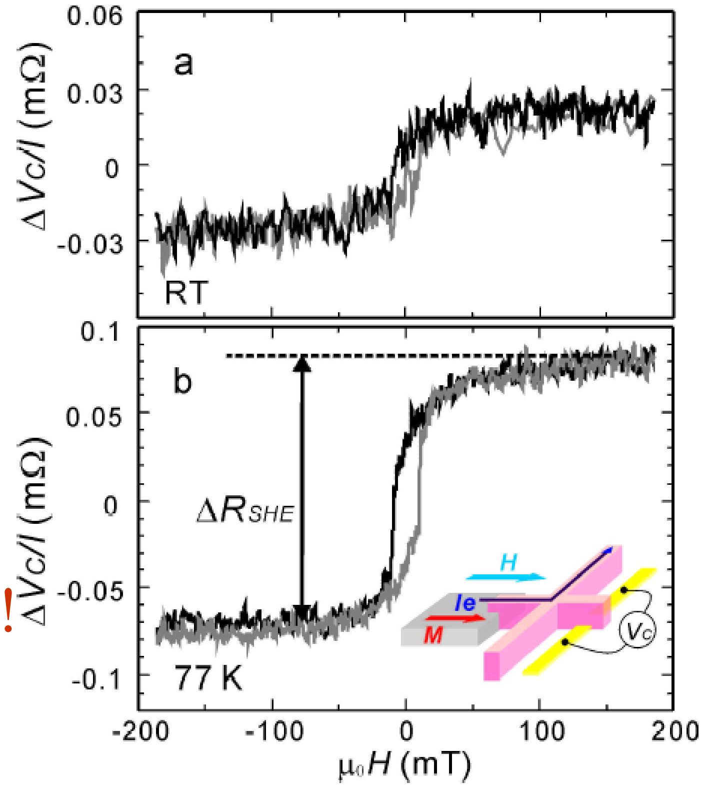

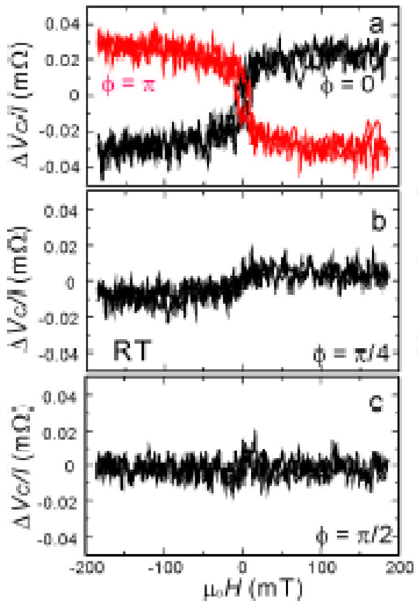

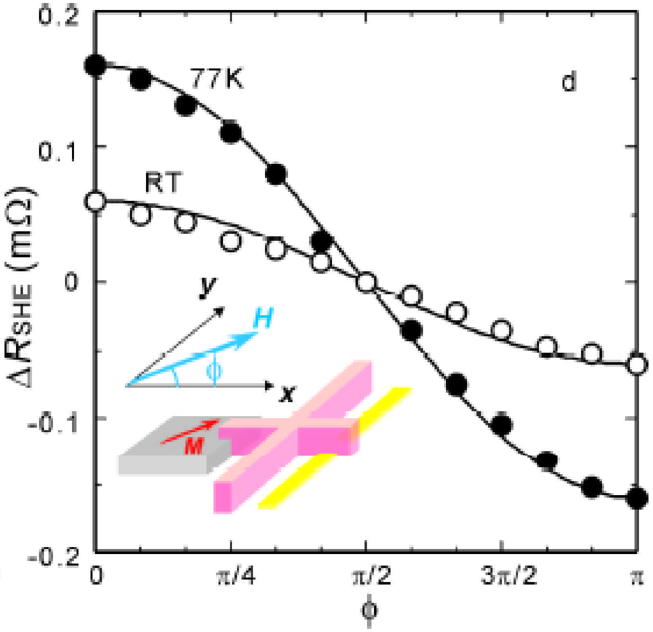

Motivations

Thus, it is important to understand the detailed mechanism of the SHE in metals because it would lead to the material design of the large SHE even at room temperature with the application to the spintronics. To this end, ab initio band theoretical calculations for real metal systems is essential.

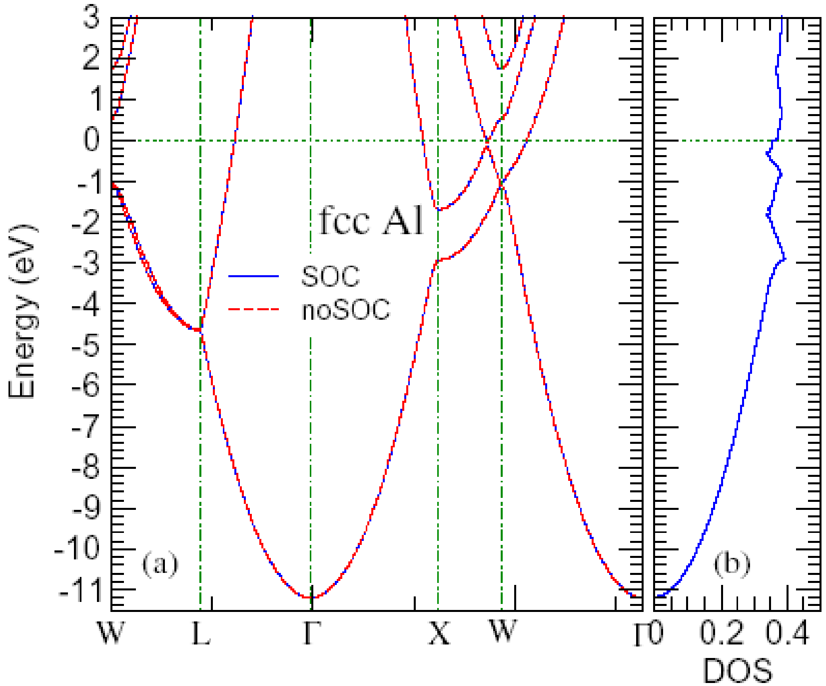

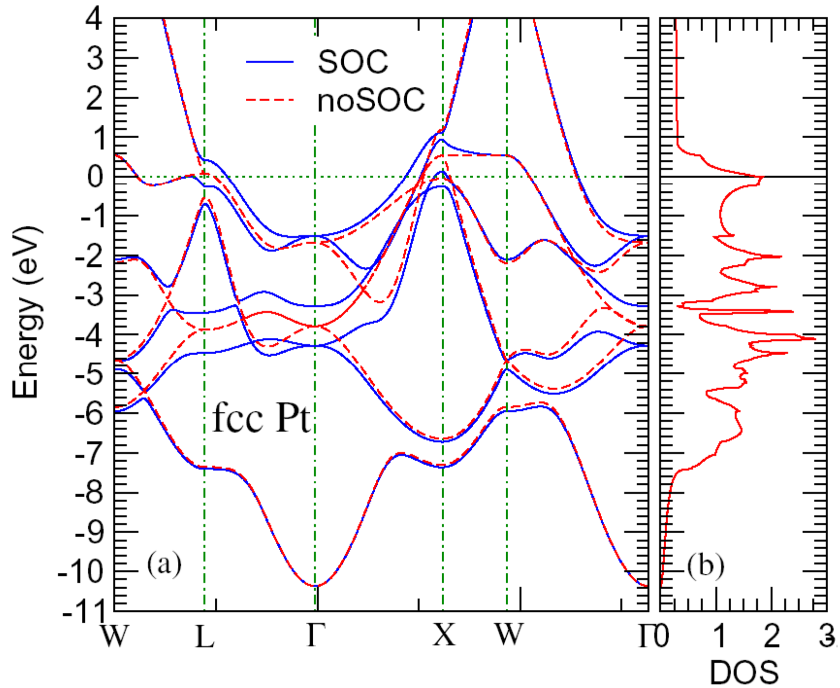

II. Intrinsic spin Hall effect in solids

1. Berry phase formalism for intrinsic Hall effects

(1) Berry phase

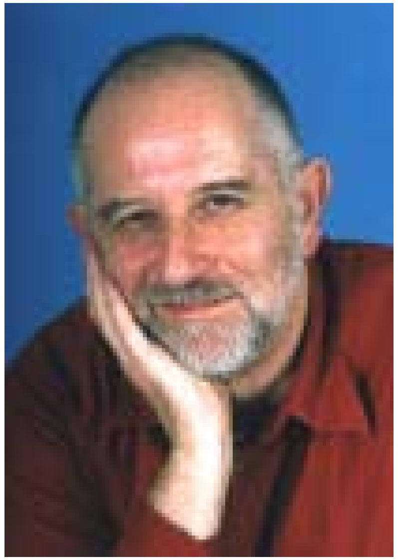

[Berry, Proc. Roy. Soc. London A 392, 451 (1984)]

Parameter dependent system:

$$\{\varepsilon_n(\lambda),\ \psi_n(\lambda)\}$$

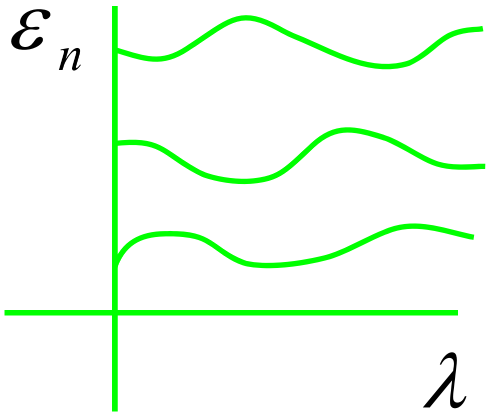

Adiabatic theorem:

$$\Psi(t) = \psi_n(\lambda(t))\ e^{-i\int_0^t dt\,\varepsilon_n/\hbar}\ e^{-i\gamma_n(t)}$$

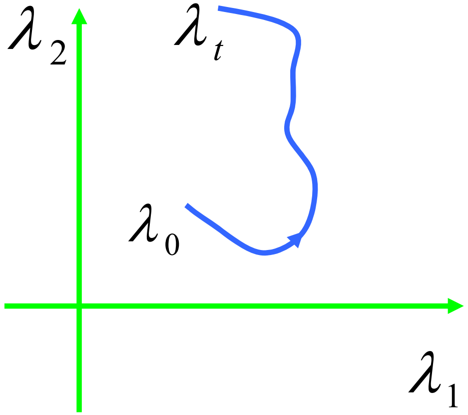

Geometric phase:

$$\gamma_n = \int_{\lambda_0}^{\lambda_t} d\lambda \left\langle \psi_n \middle| i\frac{\partial}{\partial\lambda} \middle| \psi_n \right\rangle$$

Well defined for a closed path

$$\gamma_n = \oint_C d\lambda \left\langle \psi_n \middle| i \frac{\partial}{\partial \lambda} \middle| \psi_n \right\rangle$$

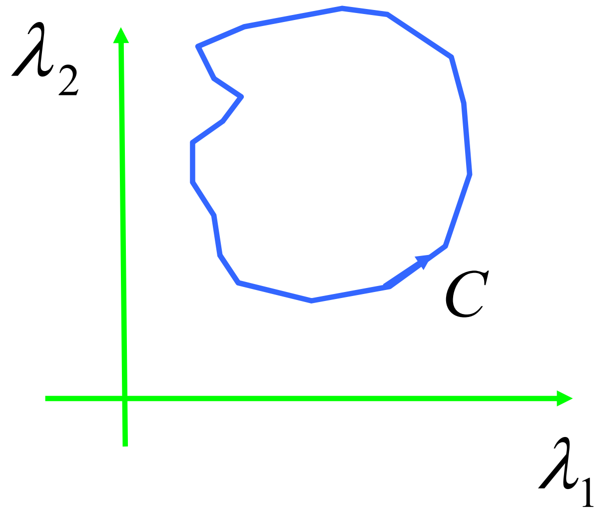

Stokes theorem

$$\gamma_n = \iint d\lambda_1 d\lambda_2 \, \Omega$$

Berry Curvature

$$\Omega = i \frac{\partial}{\partial \lambda_1} \left\langle \psi \middle| \frac{\partial}{\partial \lambda_2} \middle| \psi \right\rangle - i \frac{\partial}{\partial \lambda_2} \left\langle \psi \middle| \frac{\partial}{\partial \lambda_1} \middle| \psi \right\rangle$$

Analogies

Berry curvature

$$\Omega(\vec{\lambda})$$

Berry connection

$$\langle \psi | i \frac{\partial}{\partial \lambda} | \psi \rangle$$

Geometric phase

$$\oint d\lambda \, \langle \psi | i \frac{\partial}{\partial \lambda} | \psi \rangle = \iint d^2\lambda \;\; \Omega(\vec{\lambda})$$

Chern number

$$\oiint d^2\lambda \;\; \Omega(\vec{\lambda}) = \text{integer}$$

Magnetic field

$$B(\vec{r})$$

Vector potential

$$A(\vec{r})$$

Aharonov-Bohm phase

$$\oint dr \; A(\vec{r}) = \iint d^2 r \; B(\vec{r})$$

Dirac monopole

$$\oiint d^2 r \;\; B(\vec{r}) = \text{integer } h / e$$

(2) Semiclassical dynamics of Bloch electrons

Old version [e.g., Aschroft, Mermin, 1976]

$$\dot{\mathbf{x}}_c = \frac{1}{\hbar}\frac{\partial \varepsilon_n(\mathbf{k})}{\partial \mathbf{k}},$$

$$\dot{\mathbf{k}} = -\frac{e}{\hbar}\mathbf{E} - \frac{e}{\hbar}\dot{\mathbf{x}}_c \times \mathbf{B} = \frac{e}{\hbar}\frac{\partial \varphi(\mathbf{r})}{\partial \mathbf{r}} - \frac{e}{\hbar}\dot{\mathbf{x}}_c \times \mathbf{B}.$$

Berry phase correction [Chang & Niu, PRL (1995), PRB (1996)]

New version [Marder, 2000]

$$\dot{\mathbf{x}}_c = \frac{1}{\hbar}\frac{\partial \varepsilon_n(\mathbf{k})}{\partial \mathbf{k}} - \dot{\mathbf{k}} \times \mathbf{\Omega}_n(\mathbf{k}),$$

$$\dot{\mathbf{k}} = \frac{e}{\hbar}\frac{\partial \varphi(\mathbf{r})}{\partial \mathbf{r}} - \frac{e}{\hbar}\dot{\mathbf{x}}_c \times \mathbf{B},$$

$$\mathbf{\Omega}_n(\mathbf{k}) = -\mathrm{Im}\left\langle \frac{\partial u_{n\mathbf{k}}}{\partial \mathbf{k}} \right| \times \left| \frac{\partial u_{n\mathbf{k}}}{\partial \mathbf{k}} \right\rangle.$$ (Berry curvature)

(3) Semiclassical transport theory

$$\mathbf{j} = \int d^3k(-e\dot{\mathbf{x}})g(\mathbf{r},\mathbf{k}), \qquad g(\mathbf{r},\mathbf{k}) = f(\mathbf{k}) + \delta f(\mathbf{r},\mathbf{k})$$

$$\dot{\mathbf{x}} = \frac{\partial \varepsilon_n(\mathbf{k})}{\hbar \partial \mathbf{k}} + \frac{e}{\hbar}\mathbf{E}\times\mathbf{\Omega}$$

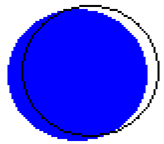

$$\mathbf{j} = -\frac{e^2}{\hbar}\mathbf{E}\times\int d^3\mathbf{k} f(\mathbf{k})\mathbf{\Omega} - \frac{e}{\hbar}\int d^3\mathbf{k}\,\delta f(\mathbf{k},\mathbf{r})\frac{\partial \varepsilon_n(\mathbf{k})}{\partial \mathbf{k}}$$

(Anomalous Hall conductance) (ordinary conductance)

Anomalous Hall conductivity [Yao, et al., PRL 92(2004) 037204]

[FLAPW (WIEN2k) calculations]

$$\sigma_{xy} = -\frac{e^2}{\hbar}\int d^3\mathbf{k}\sum_n f(\varepsilon_n(\mathbf{k}))\Omega_n^z(\mathbf{k})$$

$$\Omega_n^z(\mathbf{k}) = -\sum_{n'\neq n}\frac{2\,\mathrm{Im}\langle \mathbf{k}n|v_x|\mathbf{k}n'\rangle\langle \mathbf{k}n'|v_y|\mathbf{k}n\rangle}{(\omega_{\mathbf{k}n'}-\omega_{\mathbf{k}n})^2}$$

σ_{xy} $(\Omega\ \mathrm{cm})^{-1}$	theory	Exp.
bcc Fe	750	1030
hcp Co	443	500

3 OCTOBER 2003 VOL 302 SCIENCE www.sciencemag.org

The Anomalous Hall Effect and Magnetic Monopoles in Momentum Space

Zhong Fang,[1,2*] Naoto Nagaosa,[1,3,4] Kei S. Takahashi,[5] Atsushi Asamitsu,[1,6] Roland Mathieu,[1] Takeshi Ogasawara,[3] Hiroyuki Yamada,[3] Masashi Kawasaki,[3,7] Yoshinori Tokura,[1,3,4] Kiyoyuki Terakura[8]

Efforts to find the magnetic monopole in real space have been made in cosmic rays and in particle accelerators, but there has not yet been any firm evidence for its existence because of its very heavy mass, $\sim 10^{16}$ giga–electron volts. We show that the magnetic monopole can appear in the crystal momentum space of solids in the accessible low-energy region ($\sim$0.1 to 1 electron volts) in the context of the anomalous Hall effect. We report experimental results together with first-principles calculations on the ferromagnetic crystal $SrRuO_3$ that provide evidence for the magnetic monopole in the crystal momentum space.

D

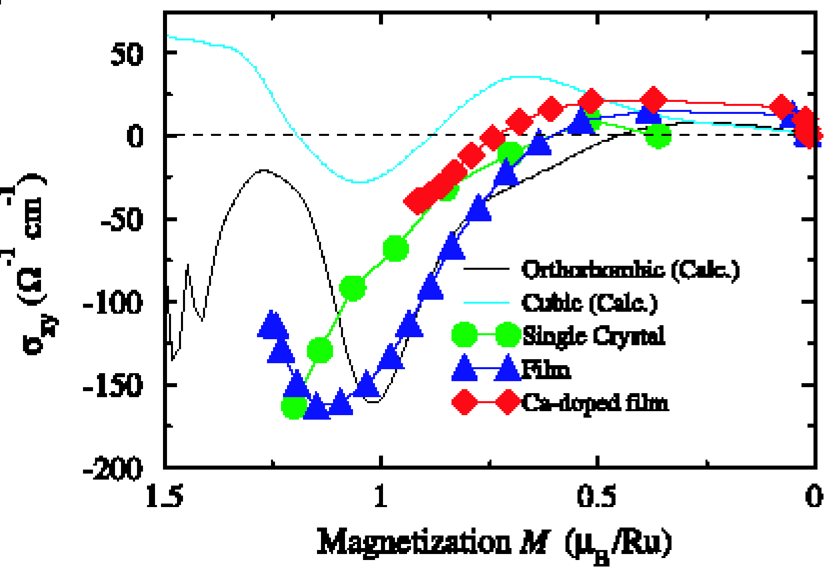

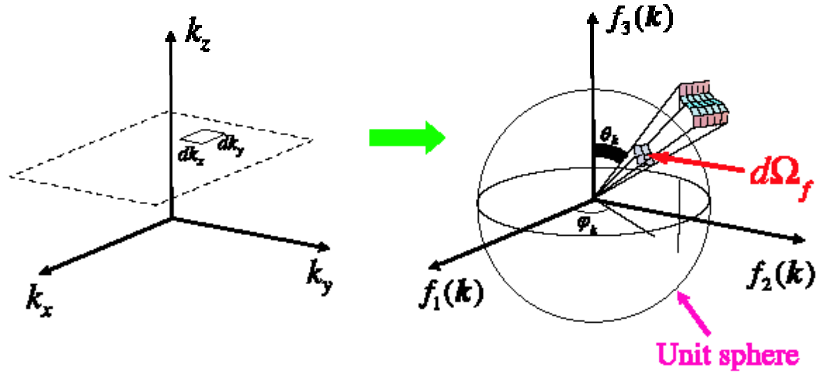

B

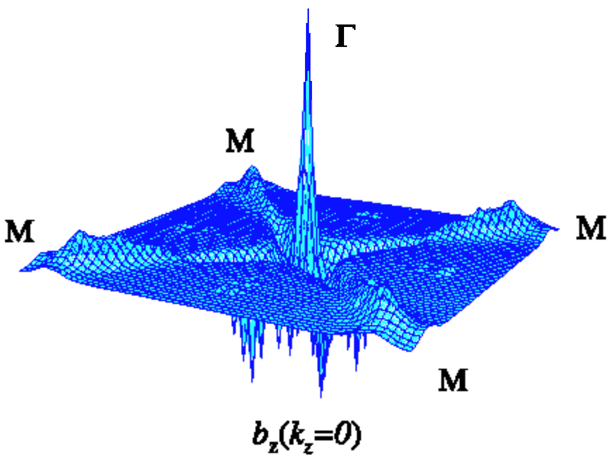

(4) *Ab initio* relativistic band structure methods

Calculations must be based on a relativistic band theory because all the intrinsic Hall effects are caused by spin-orbit coupling.

(i) Relativistic extension of linear muffin-tin orbital (LMTO) method.
[Ebert, PRB 1988; Guo & Ebert, PRB 51, 12633 (1995)]

Dirac Hamiltonian $$H_D = c\boldsymbol{\alpha}\cdot\mathbf{p} + mc^2(\beta - I) + v(\mathbf{r})I$$

$$\sigma_{xy} = \frac{e}{\hbar}\int d^3\mathbf{k}\sum_n f(\varepsilon_n(\mathbf{k}))\Omega_n^z(\mathbf{k})$$

$$\Omega_n^z(\mathbf{k}) = -\sum_{n'\neq n}\frac{2\,\mathrm{Im}\left\langle \mathbf{k}n \,|\, j_x \,|\, \mathbf{k}n'\right\rangle\left\langle \mathbf{k}n' \,|\, v_y \,|\, \mathbf{k}n\right\rangle}{(\omega_{\mathbf{k}n} - \omega_{\mathbf{k}n'})^2}$$

current operator $\mathbf{j} = -ec\alpha$ (AHE), (charge current operator)

$$\mathbf{j} = \frac{\hbar}{4}\{\beta\Sigma_z, c\alpha_i\}$$ (SHE), (spin current operator)

$$\mathbf{j} = \frac{\hbar}{2}\{\beta L_z, c\alpha\}$$ (OHE). (orbital current operator)

α, β, Σ are 4×4 Dirac matrices.

(5) Application to intrinsic spin Hall effect in semiconductors

[Guo,Yao,Niu, PRL 94, 226601 (2005)]

Spin and orbital angular momentum Hall effects in p-type zincblende semicoductors

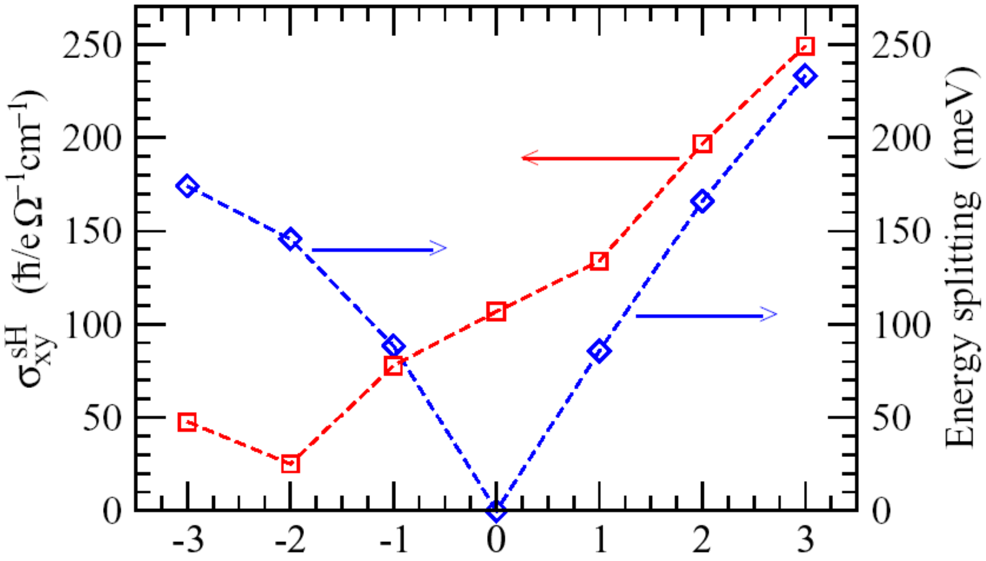

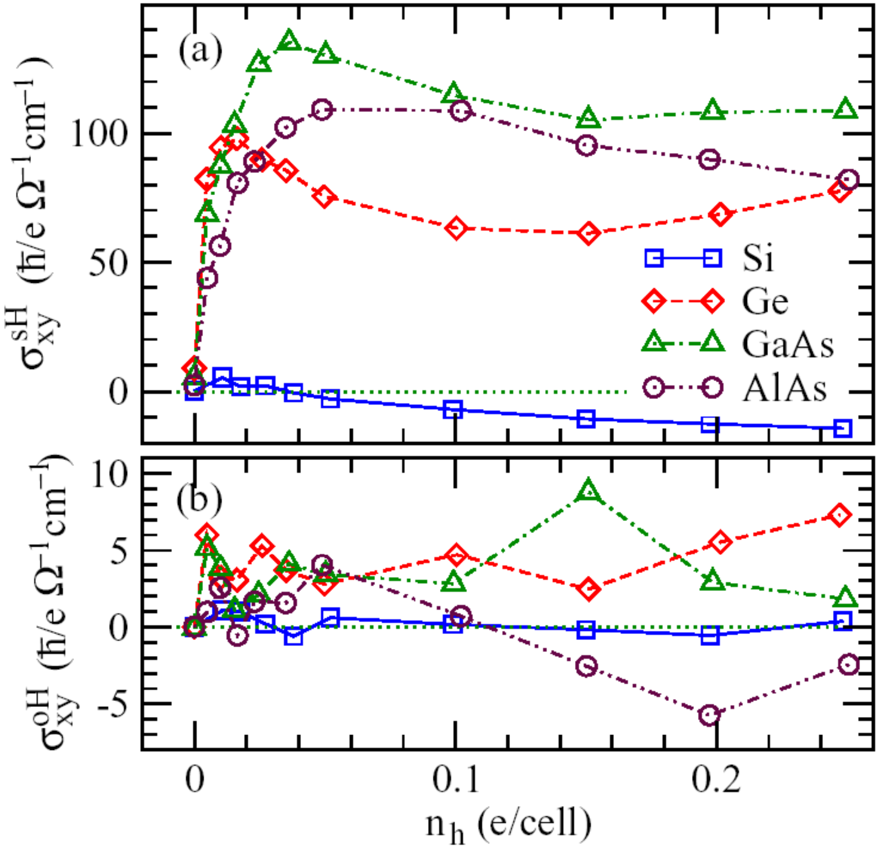

Strain effect

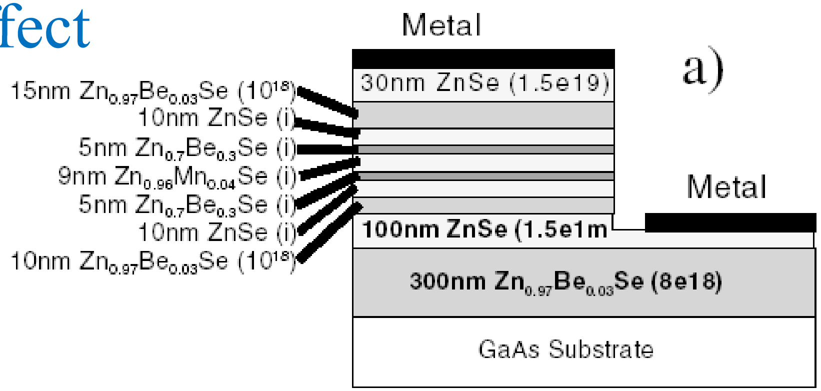

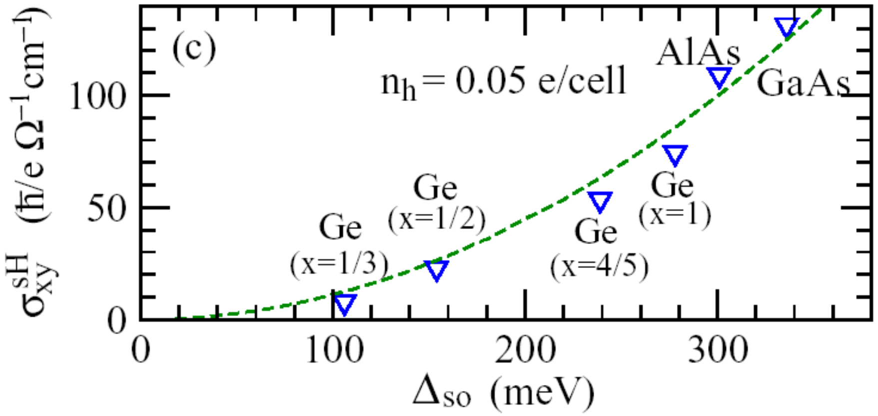

2. Large intrinsic spin Hall effect in platinum

Direct electronic measurement of the spin Hall effect

S. O. Valenzuela[1] † & M. Tinkham[1]

Nature 13 July 2006 Vol. 442,

fcc Al

$\sigma_{sH} = 27\sim34\ (\Omega\text{cm})^{-1}$
$(T = 4.2\ \text{K})$

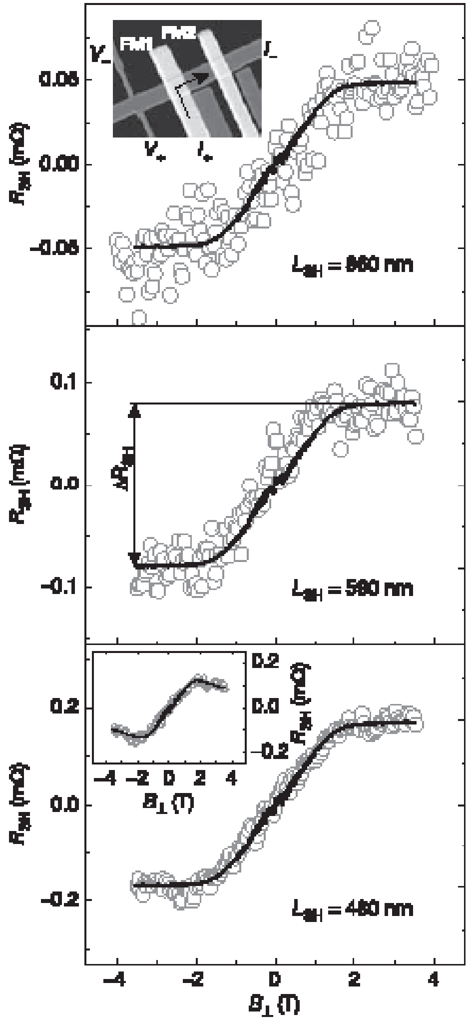

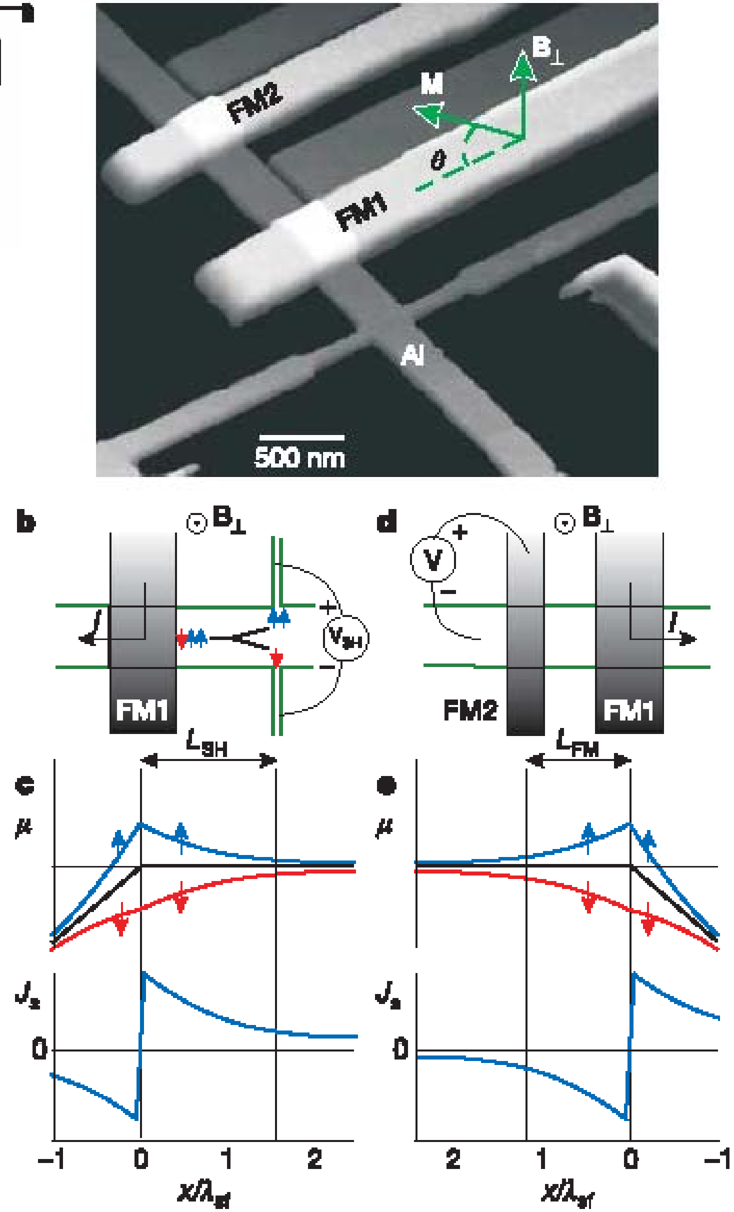

Room Temperature Reversible Spin Hall Effect

[PRL98, 156601; 98 (2007), 139901 (E) (2007)]

T. Kimura,[1,2] Y. Otani,[1,2] T. Sato,[1] S. Takahashi,[3,4] and S. Maekawa[3,4]

[1] *Institute for Solid State Physics, University of Tokyo*

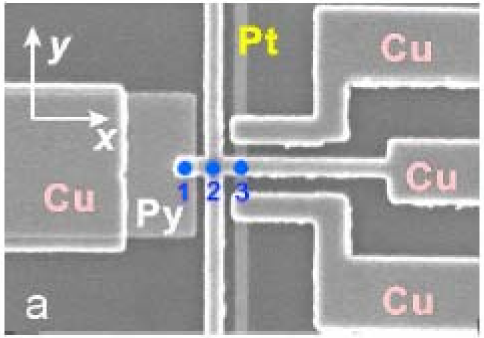

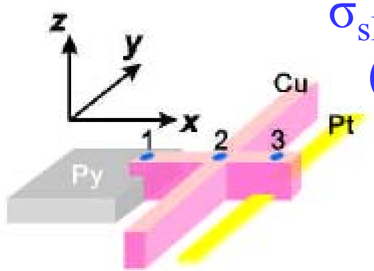

σ_{sH} = 240 $(\Omega\text{cm})^{-1}$

(T= 290 K)

Assumed to be extrinsic!

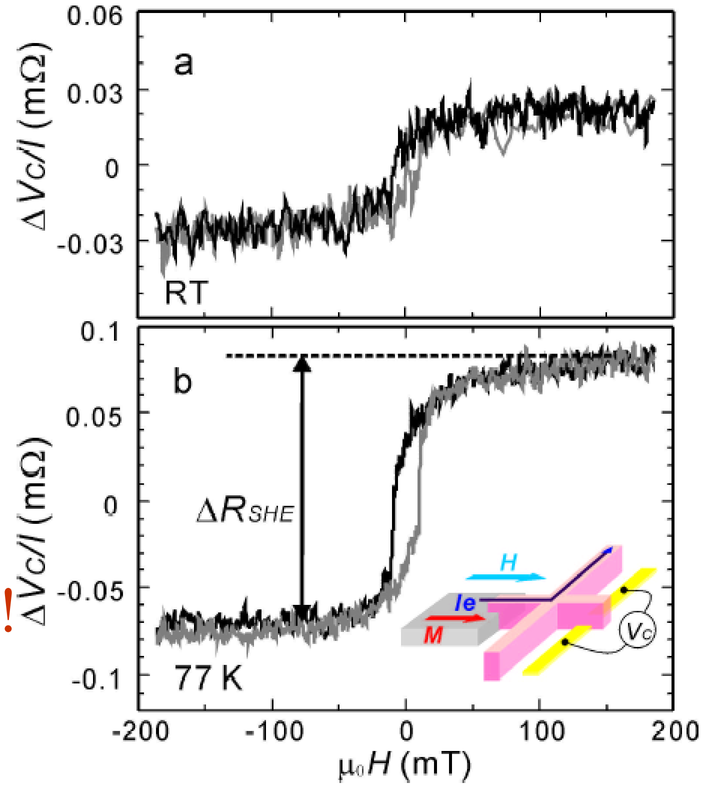

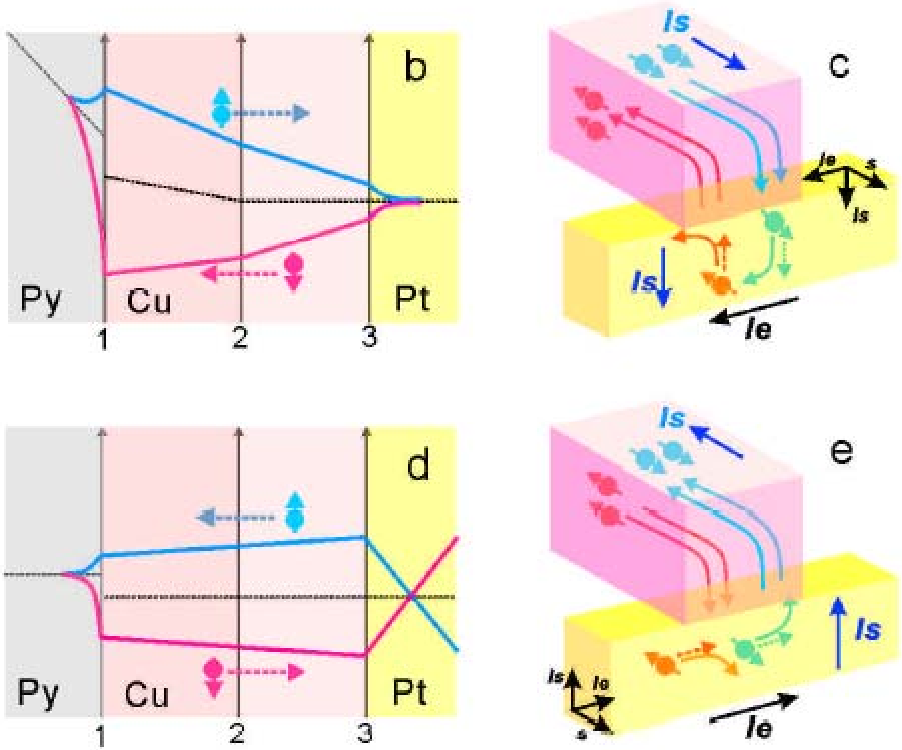

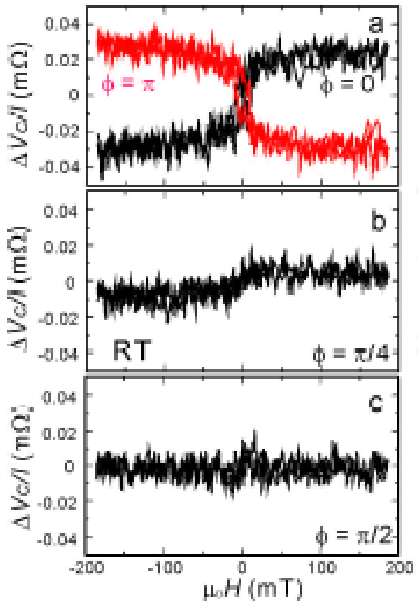

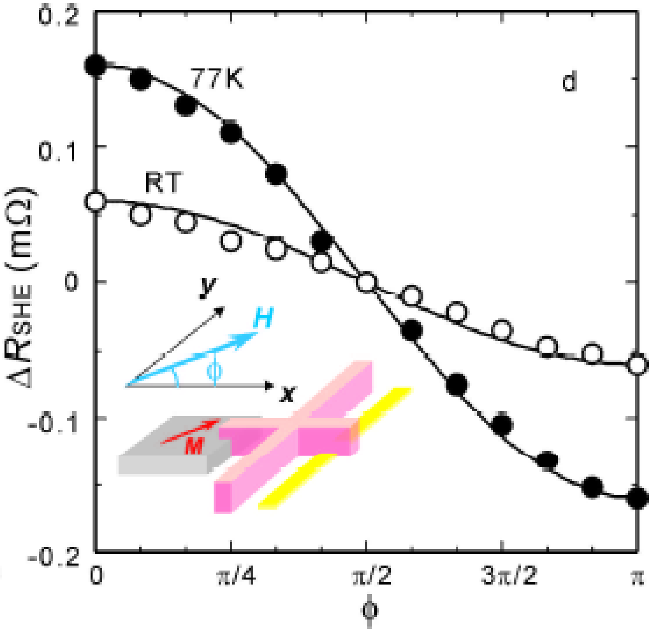

Ab initio relativistic band structure calculations

Pt: $\sigma_{sH} = 2200\ (\Omega\text{cm})^{-1}$
($T = 0$ K)

Al: $\sigma_{sH} = 17\ (\Omega\text{cm})^{-1}$
($T = 0$ K)

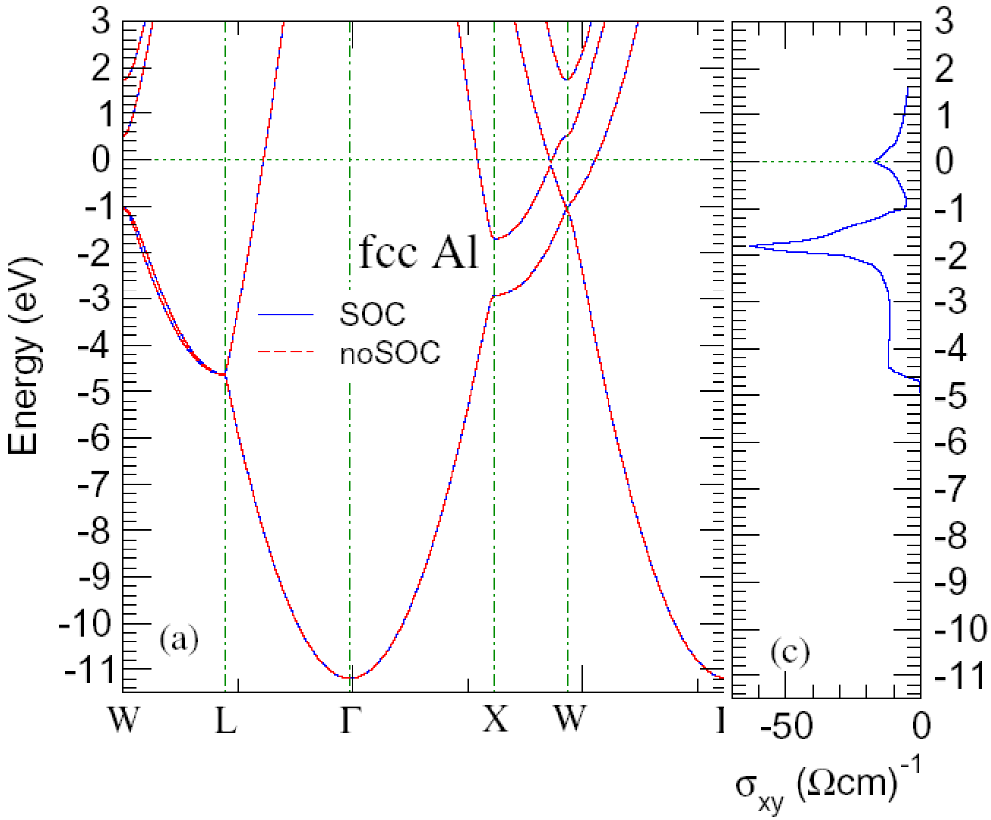

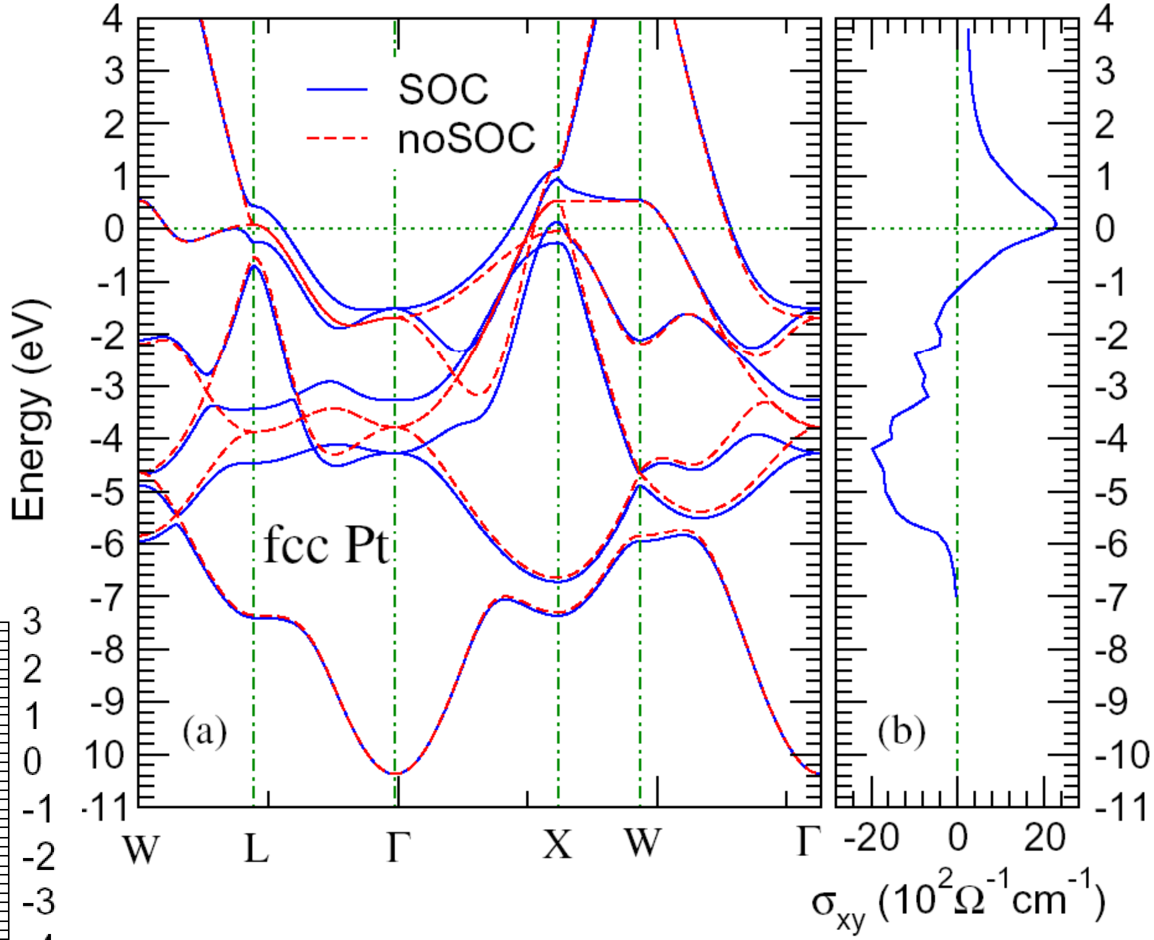

[Guo, Murakami, Chen, Nagaosa, PRL100, 096401 (2008)]

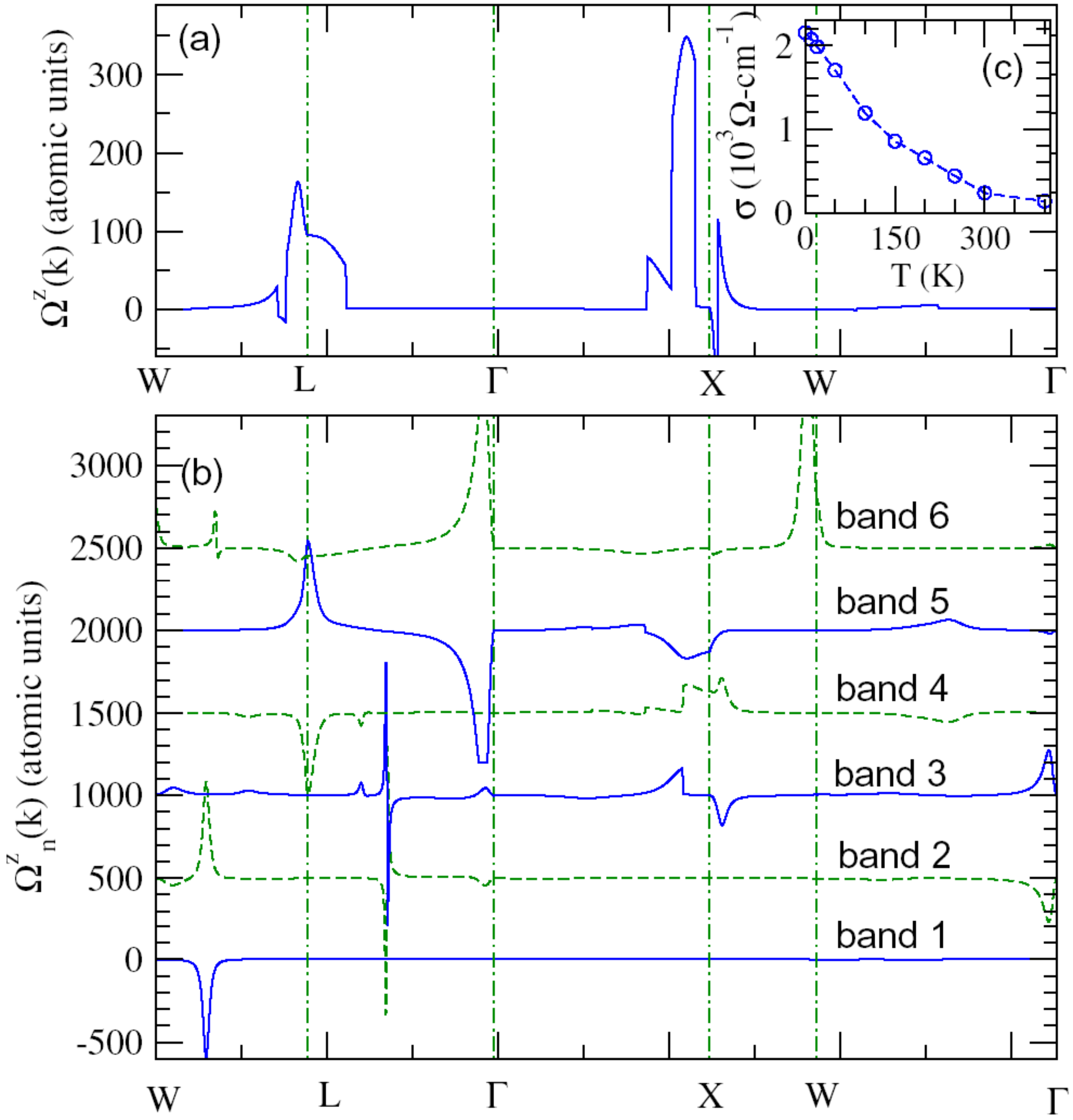

$$\sigma_{xy} = -\frac{e}{\hbar}\sum_{\mathbf{k}}\Omega^z(\mathbf{k}) = \frac{e}{\hbar}\sum_{\mathbf{k}}\sum_n f(\varepsilon_n(\mathbf{k}))\Omega^z_n(\mathbf{k})$$

$$\Omega^z_n(\mathbf{k}) = \sum_{n'\neq n}\frac{2\,\mathrm{Im}\langle \mathbf{k}n \,|\, j^z_x \,|\, \mathbf{k}n'\rangle\langle \mathbf{k}n' \,|\, v_y \,|\, \mathbf{k}n\rangle}{(\omega_{\mathbf{k}n}-\omega_{\mathbf{k}n'})^2}$$

Pt: σ_{sH} (300K) = 240 $(\Omega\mathrm{cm})^{-1}$

σ_{sH} (exp., RT) = 240 $(\Omega\mathrm{cm})^{-1}$

Al: σ_{sH} (4.2 K) = 17 $(\Omega\mathrm{cm})^{-1}$

σ_{sH} (300 K) = 6 $(\Omega\mathrm{cm})^{-1}$

σ_{sH} (exp., 4.2K) = 27, 34 $(\Omega\mathrm{cm})^{-1}$

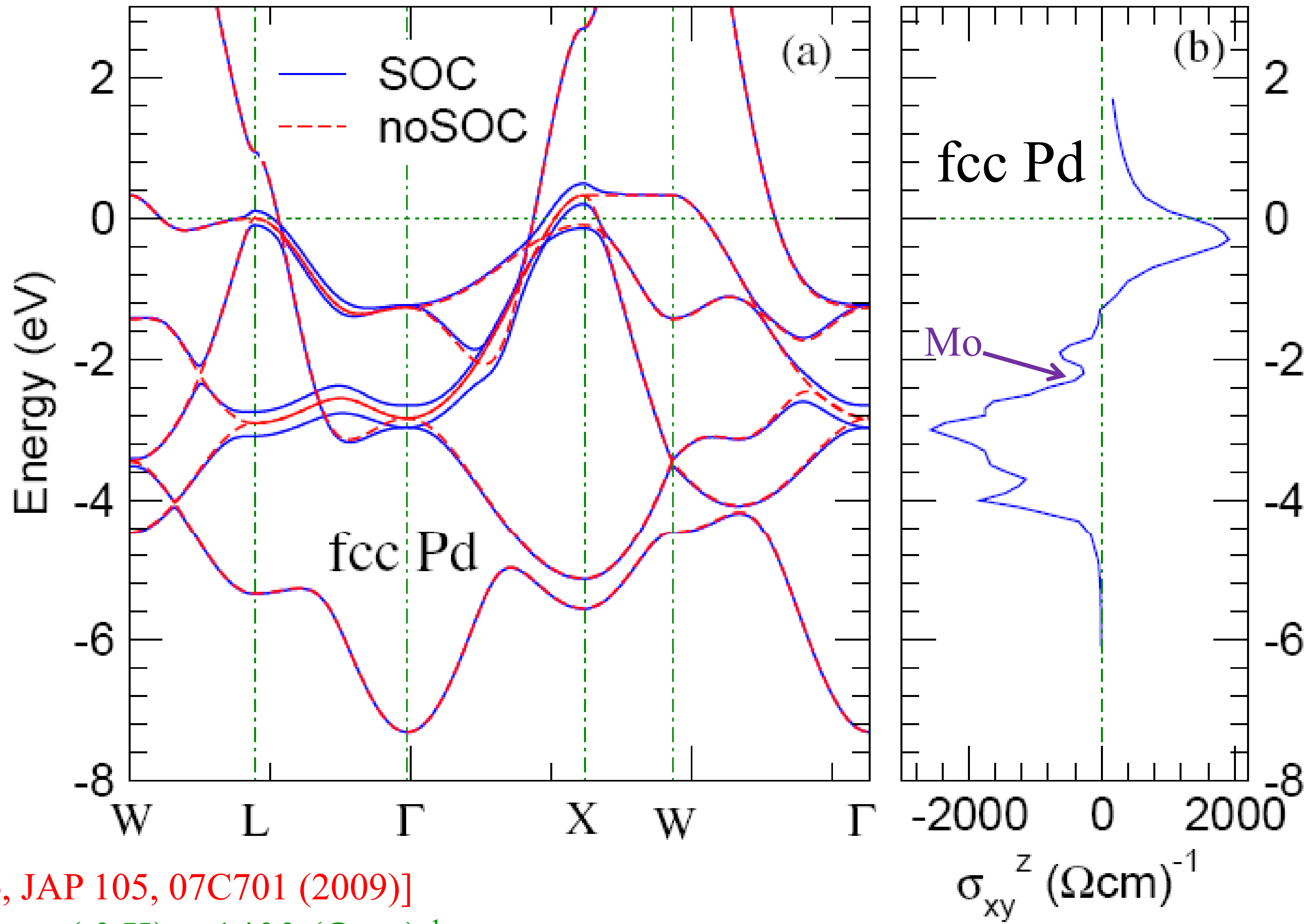

[Guo, JAP 105, 07C701 (2009)]

Pd: σ_{sH} (0 K) = 1400 $(\Omega cm)^{-1}$

σ_{sH} (300K) = 300 $(\Omega cm)^{-1}$

[Morota, et al., JAP 105, 07C712 (2009)]

Mo: σ_{sH} (10 K) = -70 $(\Omega cm)^{-1}$

α_{sH} (10K) = -0.002

III. Giantic spin Hall effect in gold and multi-orbital Kondo effect

1. Giant spin Hall effect in perpendicularly spin-polarized FePt/Au devices

[Seki, et al., Nat. Mater. 7 (2008)125]

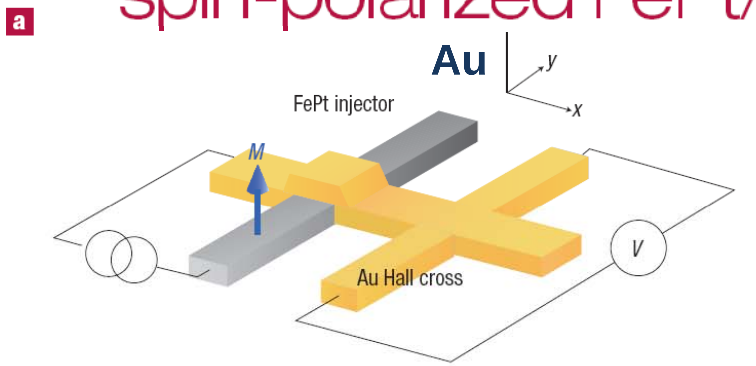

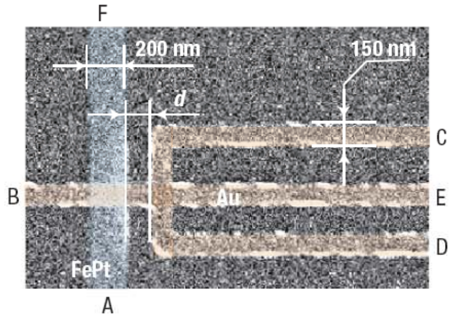

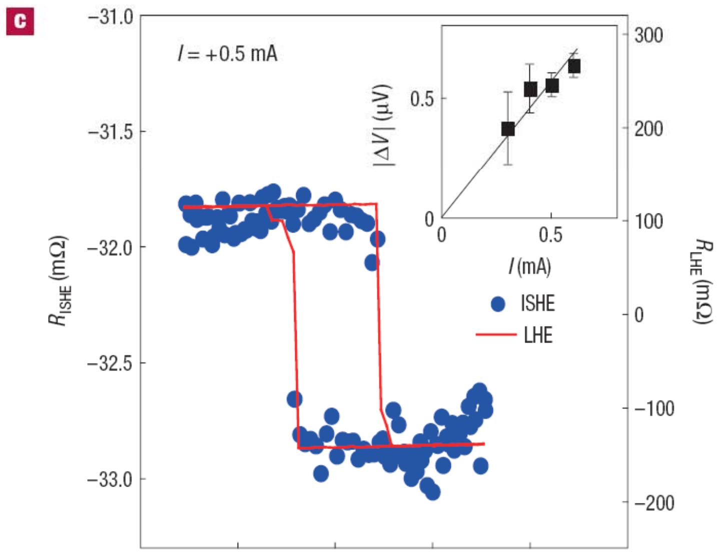

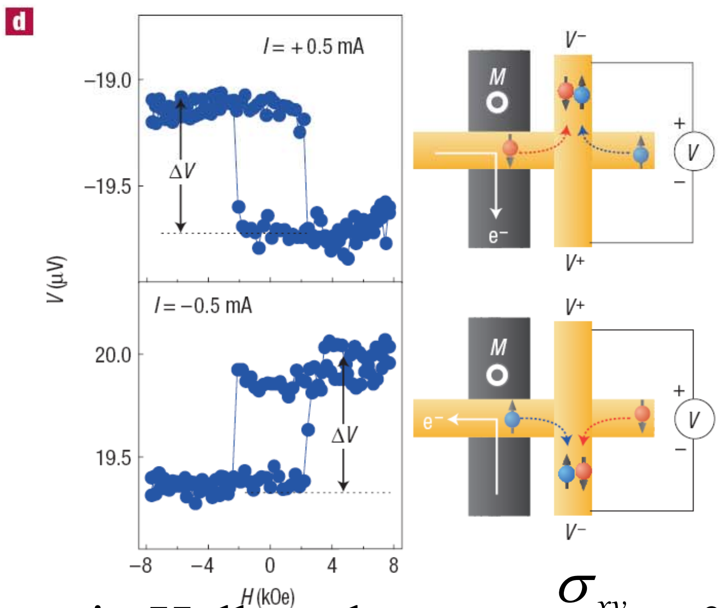

$\sigma_{SHE} \approx 10^5 \Omega^{-1}\mathrm{cm}^{-1}$

$$\Delta R_{\mathrm{ISHE}} = 2\alpha_{\mathrm{H}} \frac{\rho_{\mathrm{Au}}}{t_{\mathrm{Au}}} P \exp(-d/\lambda_{\mathrm{Au}}),$$

spin Hall angle $\alpha_H = \dfrac{\sigma_{xy}}{\sigma_{xx}} \approx 0.1$ at RT

Intrinsic spin Hall effect in pure Au metal

[Guo, JAP 105, 07C701 (2009)]

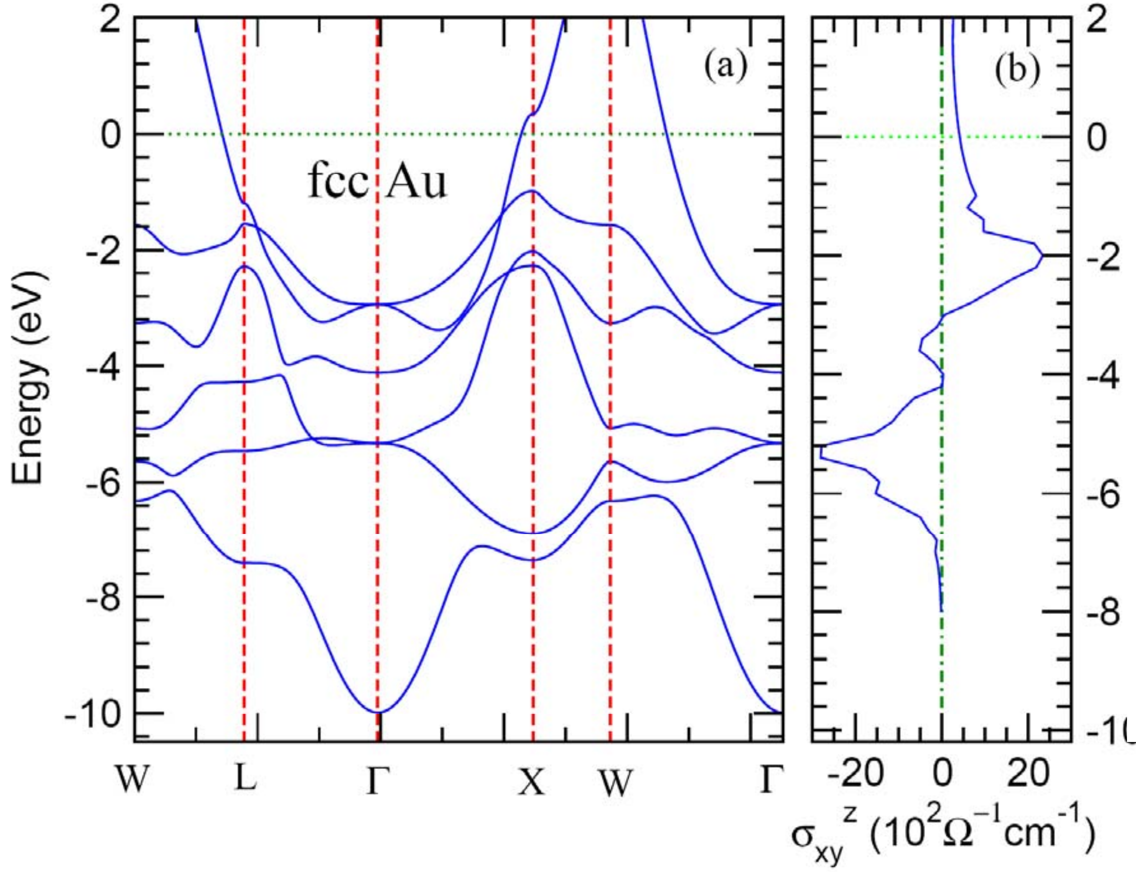

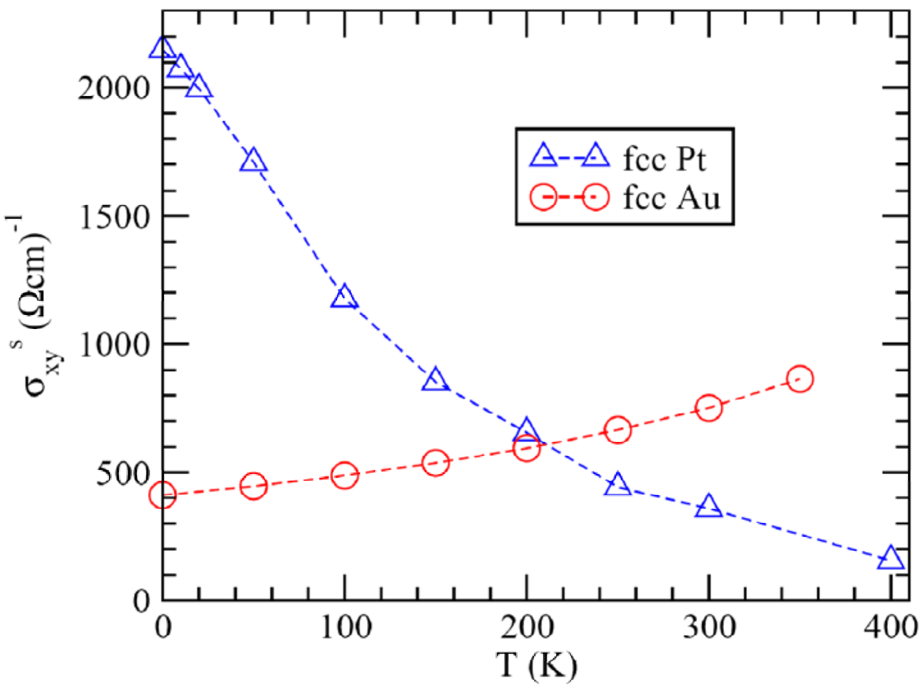

Pt: σ_{sH} = 2200 $(\Omega cm)^{-1}$
(T = 0 K)

Au: σ_{sH} = 415 $(\Omega cm)^{-1}$
(T = 0 K)

Au: σ_{sH} = 366 $(\Omega cm)^{-1}$
(T = 0 K)

[Yao & Fang, PRL95, 156601 (2005)]

Pt: σ_{sH} = 240 $(\Omega cm)^{-1}$
(T = 300 K)

Au: σ_{sH} = 750 $(\Omega cm)^{-1}$
(T = 300 K)

What is the origin of giant spin Hall effect in gold Hall bars?

(i) Surface and interface effect? [Seki, et al., Nat. Mater. 7 (2008)125]

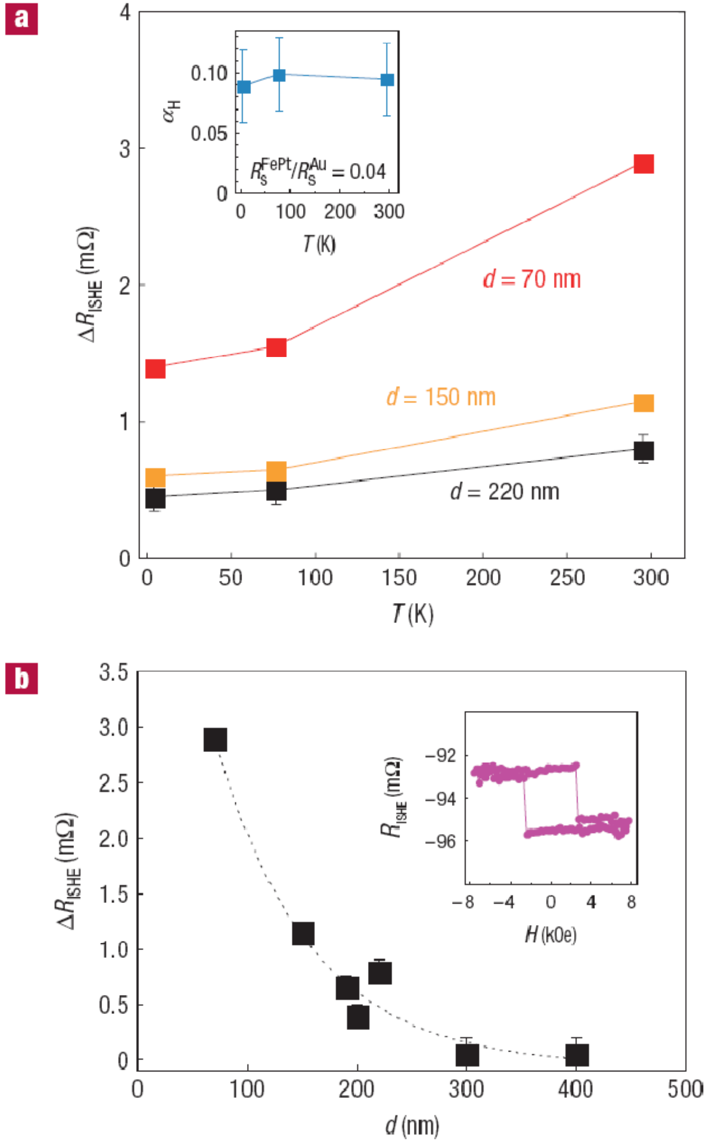

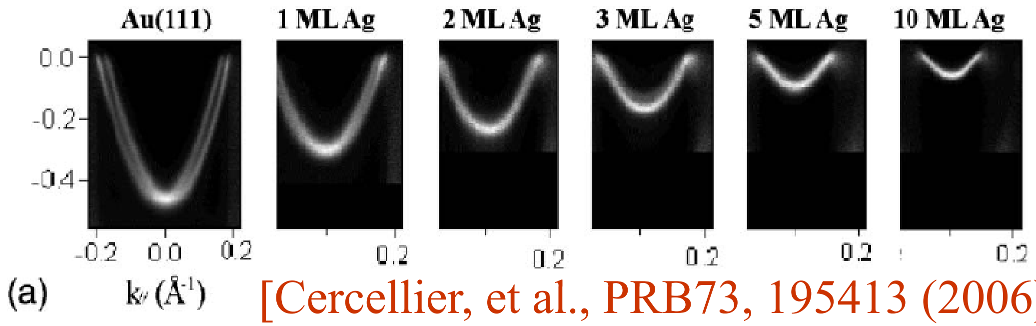

[Cercellier, et al., PRB73, 195413 (2006)]

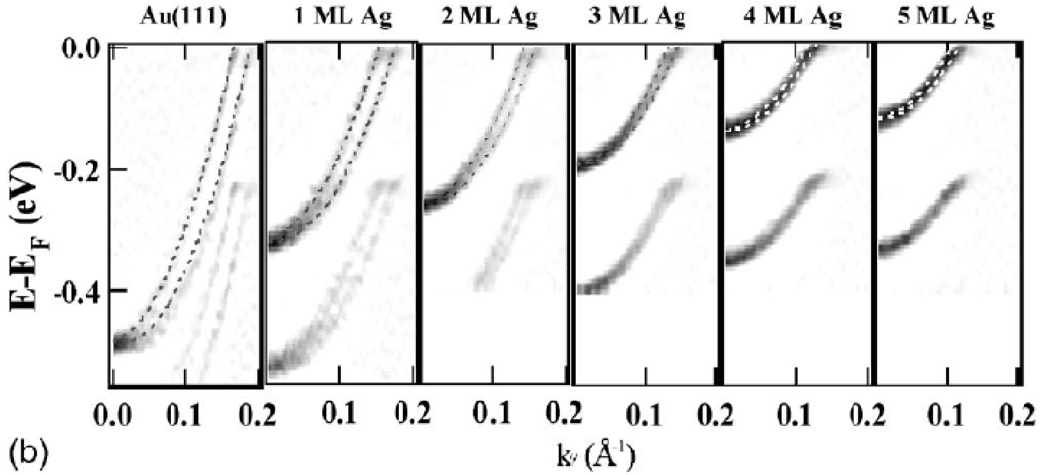

(ii) Defect and impurity origin ?

Possible impurities: (a) vacancy of Au atom
(b) Pt impurity
(c) Fe impurity

2. Multiorbital Kondo effect in Fe impurity in gold.

Results of ab initio calculations
(a) the change in DOS in the 5d bands.
(b) the DOS change is near -1.5 eV.
Nonmagnetic in (a) and (b)
(c) A peak in DOS at the Fermi level and magnetic.

Proposal: Multiorbital Kondo effect in Fe impurity in gold.

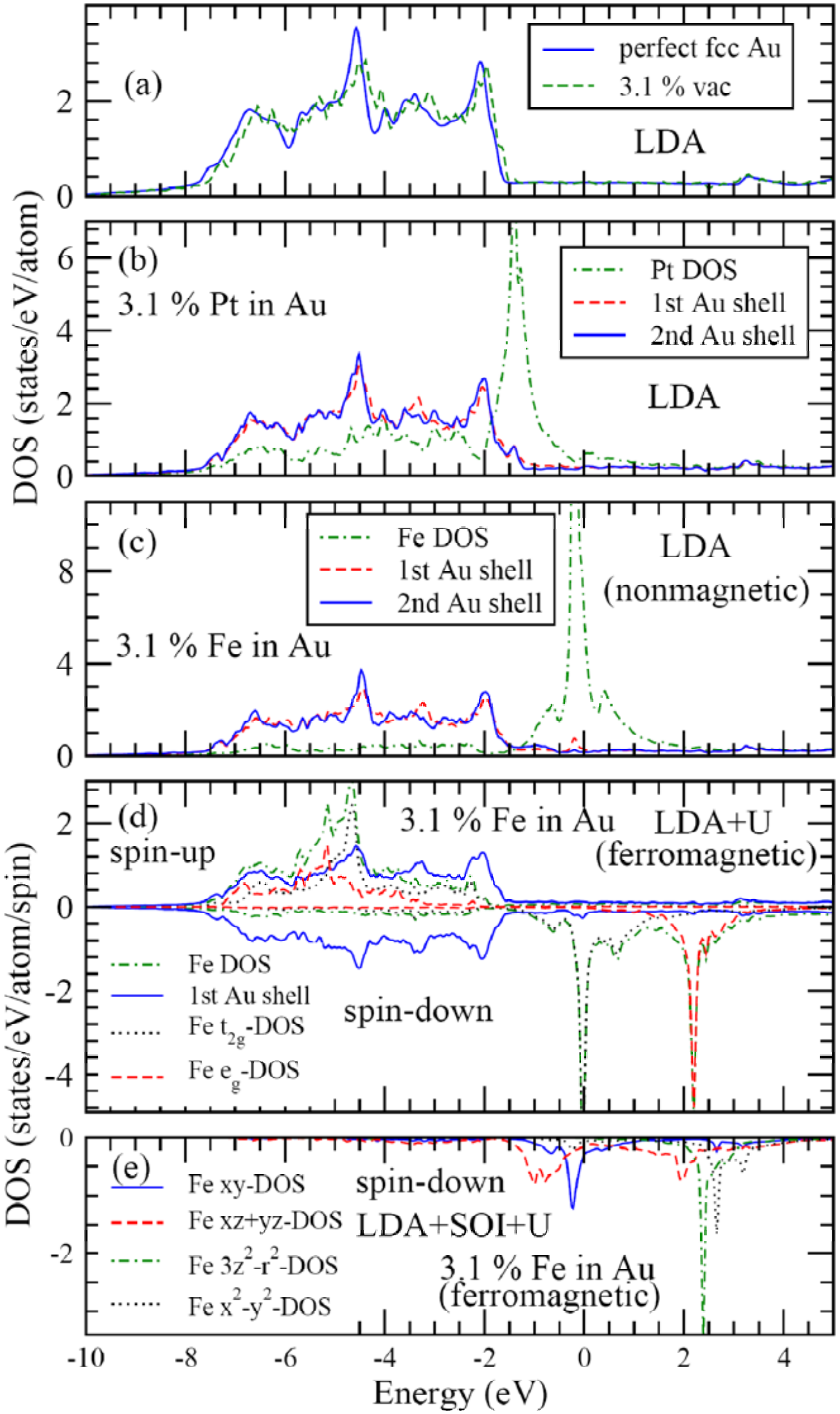

[Guo, Maekawa, Nagaosa, PRL 102, 036401 (2009)]

3. Enhanced SHE by resonant skew scattering in orbital-dependent Kondo effect.

[Guo, Maekawa, Nagaosa, PRL 102, 036401 (2009)]

Extrinsic spin Hall effect due to skew scattering

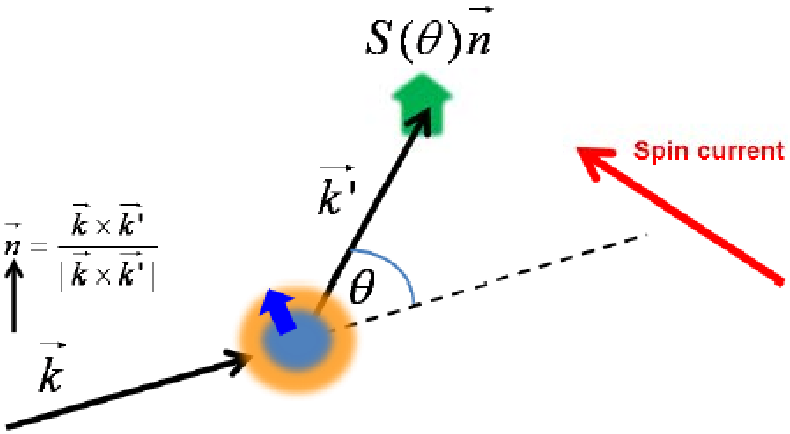

FIG. 1: (color online) The skew scattering due to the spin-orbit interaction of the scatterer and the spin unpolarized electron beam with wavevector $\vec{k}$ with the angle θ with the spin polarization $S(\theta)\vec{n}$ with $\vec{n} = (\vec{k}\times\vec{k}')/|\vec{k}\times\vec{k}'|$.

scattering amplitudes

$$\begin{aligned} f_\uparrow(\theta) &= f_1(\theta)|\uparrow\rangle + ie^{i\varphi} f_2(\theta)|\downarrow\rangle \\ f_\downarrow(\theta) &= f_1(\theta)|\downarrow\rangle - ie^{-i\varphi} f_2(\theta)|\uparrow\rangle \end{aligned}$$

skewness function

$$S(\theta) = \frac{2\mathrm{Im}[f_1^*(\theta) f_2(\theta)]}{|f_1(\theta)|^2 + |f_2(\theta)|^2}$$

spin Hall angle

$$\gamma_S = \frac{\int d\Omega I(\theta) S(\theta)\sin\theta}{\int d\Omega I(\theta)(1-\cos\theta)}$$

$$\begin{aligned} f_1(\theta) &= \sum_l \frac{P_l(\cos\theta)}{2ik}\left[(l+1)\left(e^{2i\delta_l^+}-1\right) + l\left(e^{-2i\delta_l^-}-1\right)\right] \\ f_2(\theta) &= \sum_l \frac{\sin\theta}{2ik}\left(e^{2i\delta_l^+} - e^{2i\delta_l^-}\right)\frac{d}{d\cos\theta}P_l(\cos\theta). \end{aligned}$$

TABLE I: Down-spin occupation numbers of the $3d$-suborbitals of the Fe impurity in Au from LDA+U calculations without SOI and with SOI. The calculated magnetic moments are: $m_s^{Fe} = 3.39\ \mu_B$ and $m_s^{tot} = 3.32\ \mu_B$ without SOI, as well as $m_s^{Fe} = 3.19\ \mu_B$, $m_o^{Fe} = 1.54\ \mu_B$ and $m_s^{tot} = 3.27\ \mu_B$ with SOI. The muffin-tin sphere radius $R_{mt} = 2.65 a_0$ (a_0 is Bohr radius) is used for both Fe and Au atoms.

[Guo, Maekawa, Nagaosa, PRL 102, 036401 (2009)]

(a)	xy	xz	yz	$3z^2-r^2$	x^2-y^2
no SOI	0.459	0.459	0.459	0.053	0.053
SOI	0.559	0.453	0.453	0.050	0.128
(b)	$m=-2$	$m=-1$	$m=0$	$m=1$	$m=2$
no SOI	0.256	0.459	0.053	0.459	0.256
SOI	0.138	0.087	0.050	0.819	0.549

Occupation numbers are related to the phase shifts through generalized Friedel sum rule.

$$\gamma_s \cong -\frac{3\delta_1(\cos 2\delta_2^+ - \cos 2\delta_2^-)}{9\sin^2\delta_2^+ + 4\sin^2\delta_2^- + 3[1-\cos 2(\delta_2^+ - \delta_2^-)]}$$

$$\gamma_s \cong \delta_1 \approx 0.1$$

$$\gamma_H \approx 0.001 \sim 0.01$$

[Fert, et al., JMMM 24 (1981) 231]

Prediction: Large SHE would also occur in 5d impurities in Au or Ag

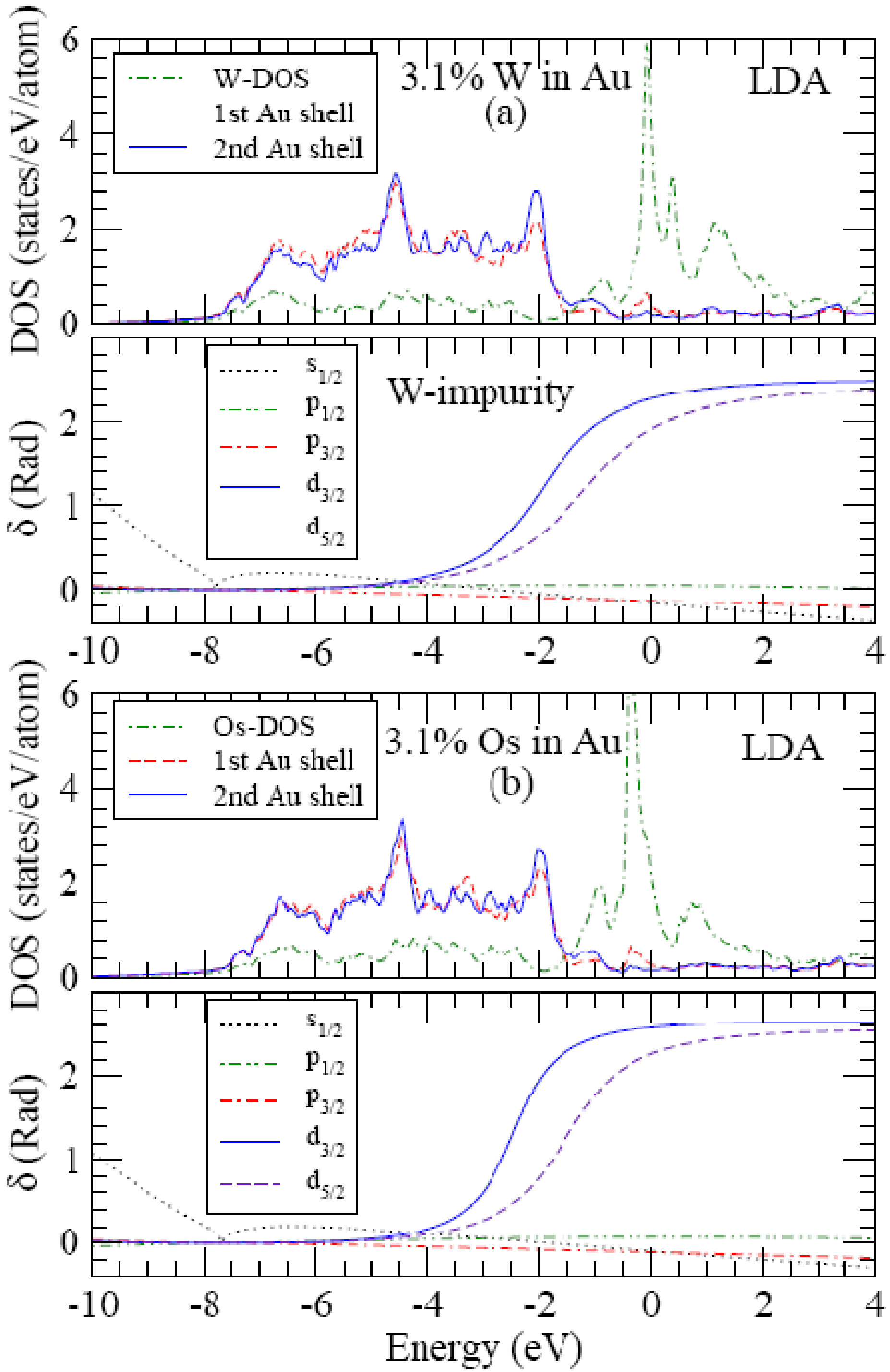

4. Quantum fluctuation in a Kondo system and QMC simulation

1) problems

PRL **102**, 036401 (2009)
Selected for a Viewpoint in *Physics*
PHYSICAL REVIEW LETTERS
week ending 23 JANUARY 2009

Enhanced Spin Hall Effect by Resonant Skew Scattering in the Orbital-Dependent Kondo Effect

Guang-Yu Guo,[1] Sadamichi Maekawa,[2,3] and Naoto Nagaosa[4,5,*]

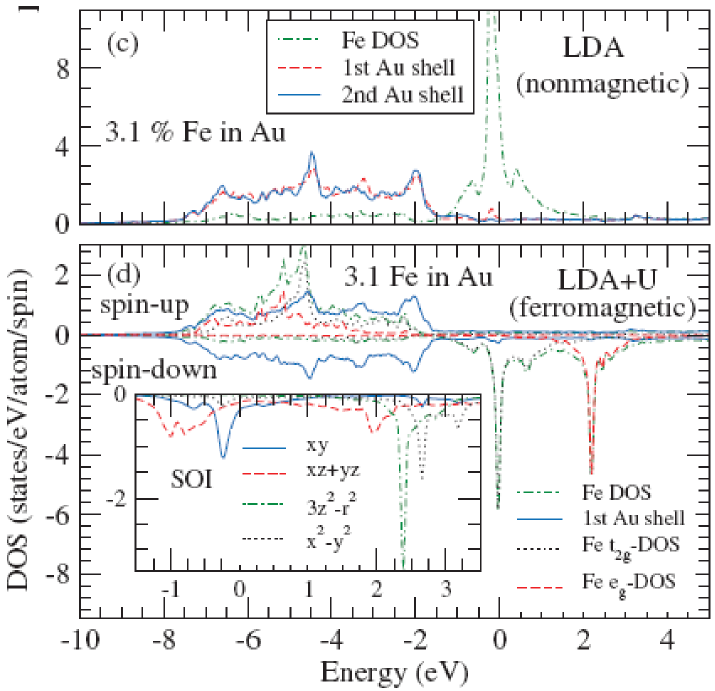

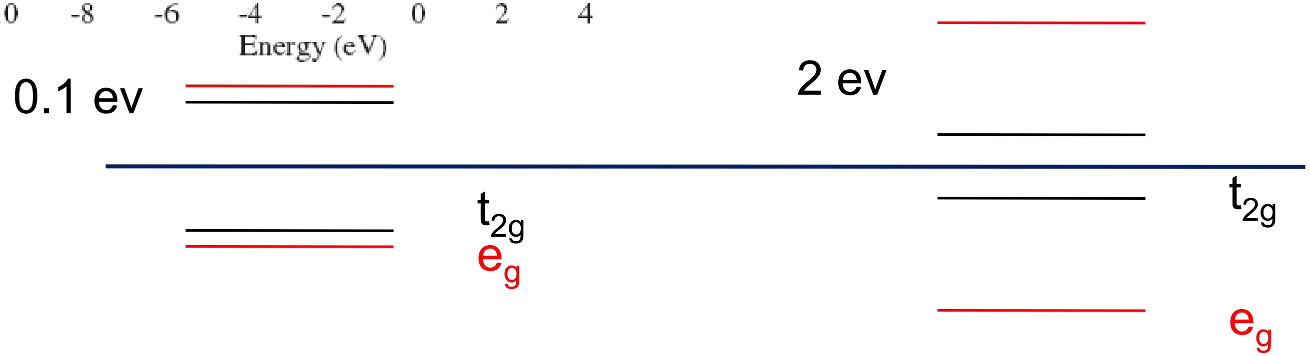

Mixed valence
T_k > R.T.

Kondo
T_k ~ 0.4 K

U = 0

U = 5 eV

Physics Physics 2, 6 (2009)
Physics 2, 6 (20

Viewpoint

Lending an iron hand to spintronics

Piers Coleman
Department of Physics and Astronomy, Rutgers University, 136 Frelinghuysen Road, Piscataway, NJ 08854-8019, USA
Published January 20, 2009

Subject Areas: Spintronics

A Viewpoint on:
Enhanced Spin Hall Effect by Resonant Skew Scattering in the Orbital-Dependent Kondo Effect
Guang-Yu Guo, Sadamichi Maekawa and Naoto Nagaosa
Phys. Rev. Lett. **102**, 036401 (2009) – Published January 20, 2009

Despite its long history, the detailed Kondo physics of iron remains a controversial subject, in part because of the complex orbital structure of the impurity atom. The magnetism of iron in gold is carried by iron's five valence d electrons, each of which resides in one of five different d orbitals. On an isolated Fe atom, these d orbitals are nearly degenerate, but in the cubic environment of the gold crystal, the d orbitals split up into two components—a doublet, labeled the e_g orbitals, and a triplet, labeled the t_{2g} orbitals. During the past year, both Guo *et al.* and a research collaboration of Theo Costi, Achim Rosch, and coworkers [11] have independently proposed that the Kondo effect in iron is "orbitally selective," involving two widely different Kondo temperatures—one for each set of orbitals. Both groups suggest that some of the iron d-spins delocalize because of the Kondo effect at room temperature, leaving behind two or three remaining electrons that only delocalize around 1 K.

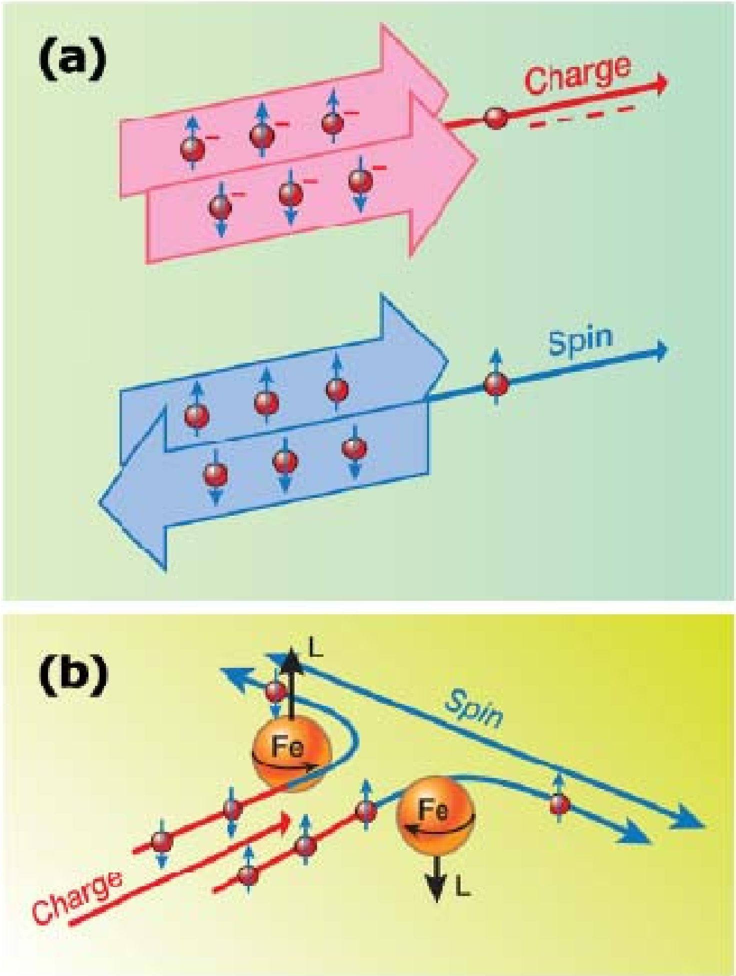

FIG. 1: (a) In a charge current, spin "up" and "down" electrons flow together. In a spin current, up and down electrons flow in opposite directions. (b) A schematic of the spin Hall effect. Spin-orbit coupling induces an orbital motion opposite in direction to the electron spin, deflecting up- and down-spin electrons in opposite directions. The net effect is a conversion of charge into spin currents. (Illustration: Alan Stonebraker/stonebrakerdesignworks.com)

PRL **102,** 056802 (2009) PHYSICAL REVIEW LETTERS week ending 6 FEBRUARY 2009

Kondo Decoherence: Finding the Right Spin Model for Iron Impurities in Gold and Silver

T. A. Costi,[1,2] L. Bergqvist,[1] A. Weichselbaum,[3] J. von Delft,[3] T. Micklitz,[4,7] A. Rosch,[4] P. Mavropoulos,[1,2] P. H. Dederichs,[1] F. Mallet,[5] L. Saminadayar,[5,6] and C. Bäuerle[5]

suggests an effective 3-channel Kondo model

$$H = \sum_{k\alpha\sigma} \varepsilon_k c^{\dagger}_{k\alpha\sigma} c_{k\alpha\sigma} + J \sum_{\alpha} \mathbf{S} \cdot \mathbf{s}_{\alpha}.$$

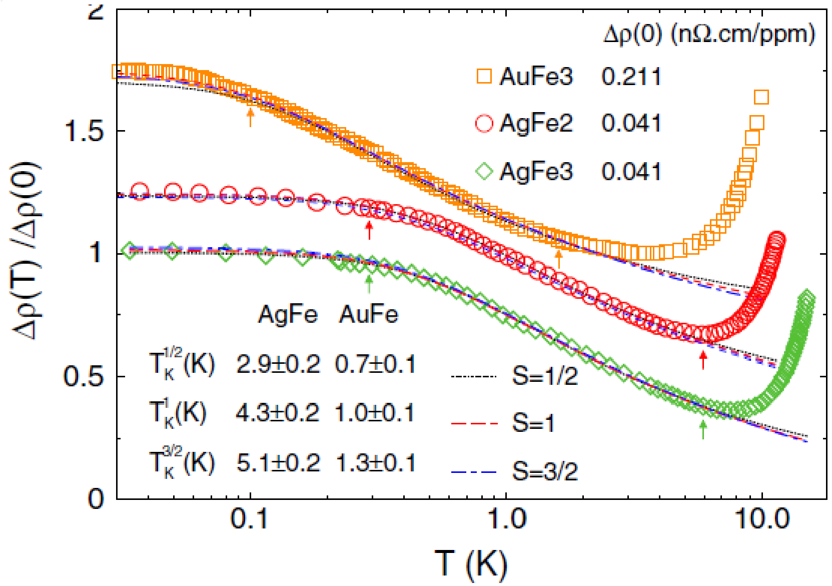

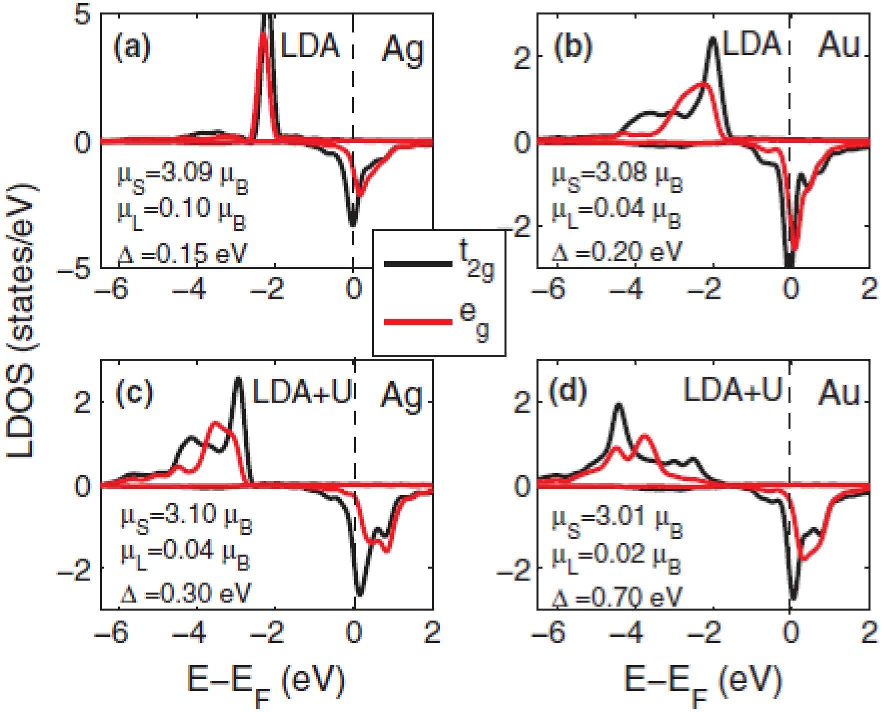

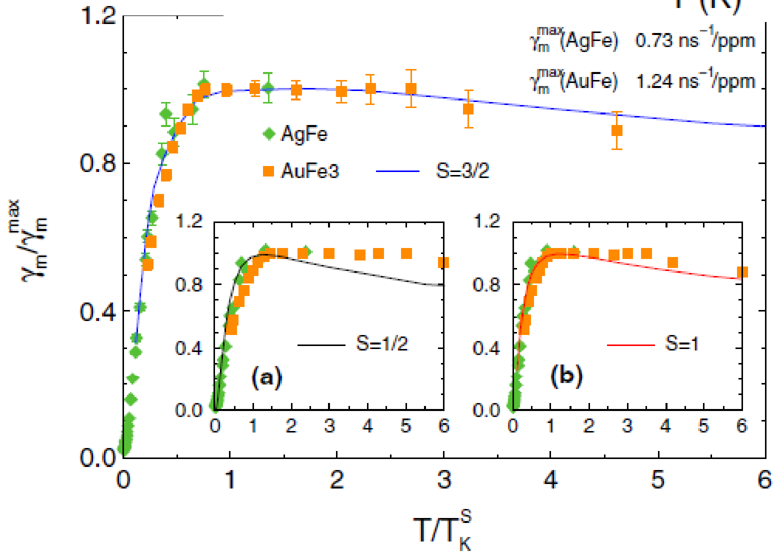

XMCD measurements

Direct Observation of Orbital Magnetism in Cubic Solids

W. D. Brewer,[1,*] A. Scherz,[1] C. Sorg,[1] H. Wende,[1] K. Baberschke,[1] P. Bencok,[2] and S. Frota-Pessôa[3]
[1]*Institut für Experimentalphysik, Freie Universität Berlin, Arnimallee 14, D-14195 Berlin-Dahlem, Germany*
[2]*European Synchrotron Radiation Facility, BP 220, F-38043 Grenoble Cedex, France*
[3]*Instituto de Física, Universidade de São Paulo, CP 66318, 05315-970 São Paulo, São Paulo, Brazil*
(Received 17 September 2003; published 11 August 2004)

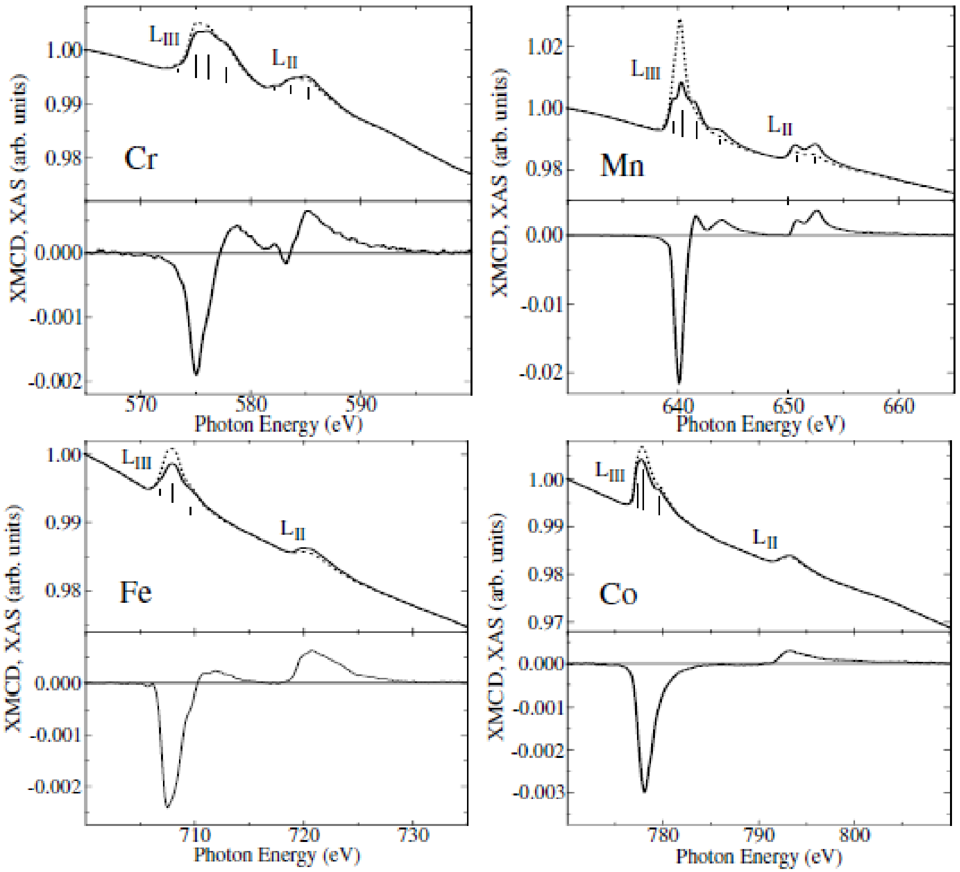

TABLE I. Experimental values of R and the derived orbital/spin magnetic moment ratios for $3d$ impurities in noble metals. The applied field was 7 T, and temperatures T are in K.

Alloy	R	T	$\mu_l/\mu_s^{\mathrm{eff}}$
*Au*Cr (1.0 at. %)	−1.01	18.7	−0.003(30)
*Au*Mn (1.0 at. %)	−0.90	6.8	+0.023(20)
*Cu*Mn (1.0 at. %)	−0.94	6.8	+0.013(20)
*Au*Fe (0.8 at. %)	−0.86	7.2	+0.034(15)
*Au*Co (1.5 at. %)	−0.247	6.8	+0.336(52)

2) Quantum Monte Carlo simulation

[Gu, Gan, Bulut, Ziman, Guo, Nagaosa, Maekawa, PRL105 (2009) 086401]

(1) Single-impurity multi-orbital Anderson Model

A realistic Anderson model is formulated with the host band structure and the impurity-host hybridization determined by ab initio DFT-LDA calculations.

$$H = \sum_{\alpha,k,\sigma} \varepsilon_{\alpha k} c^{+}_{\alpha k\sigma} c_{\alpha k\sigma} + \sum_{\xi,\sigma} \varepsilon_{\xi} d^{+}_{\xi\sigma} d_{\xi\sigma} + \sum_{\alpha,k,\xi,\sigma} \left(V_{\alpha k\xi} c^{+}_{\alpha k\sigma} d_{\xi\sigma} + h.c. \right)$$

$$+ U \sum_{\xi} n_{\xi\uparrow} n_{\xi\downarrow} + U' \sum_{\sigma,\sigma'} n_{1\sigma} n_{2\sigma'} - J \sum_{\sigma} n_{1\sigma} n_{2\sigma}$$

For host band structure, α = 9 bands (6s, 6p, 5d orbitals of Au) are included.
For impurity-host hybridization, $Au_{26}Fe$ supercell (3X3X3 primitive FCC cell) is considered. $\xi = 5$ (3d orbitals of Fe).

For impurity Fe, one e_g orbital (z^2) and one t_{2g} orbital (xz) are considered with the following parameters.

U = 5 eV, J = 0.9 eV, U'= U – 2J = 3.2 eV

Impurity-host hybridization for fcc $Au_{26}Fe$ (DFT-LDA results)

$$V_{\xi\alpha k} = \langle \varphi_\xi | H_0 | \Psi_\alpha(k) \rangle$$
$$= \sum_p a_{\alpha p}(k) \frac{1}{\sqrt{N}} \sum_r e^{ik\cdot r} \langle \varphi_\xi | H_0 | \varphi_p(r) \rangle$$
$$= \frac{1}{\sqrt{N}} \sum_{p,r} e^{ik\cdot r} a_{\alpha p}(k) \langle \varphi_\xi | H_0 | \varphi_p(r) \rangle$$

For FCC $Au_{26}Fe$:
α, p = 9 (6s, 6p, 5d orbitals of Au)
r = 26 (Au_{26})
ξ = 5 (3d orbitals of Fe)

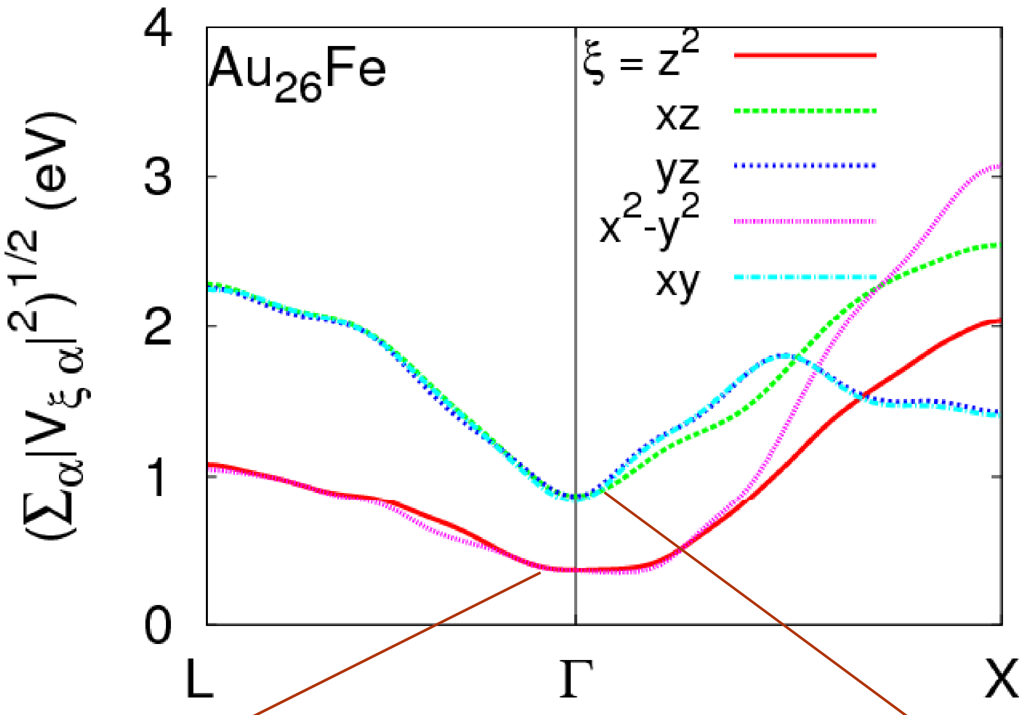

❑Energy levels for Fe in $Au_{26}Fe$ (DFT results):

t_{2g} : xz, yz, xy : -0.45 eV
e_g : z^2, x^2-y^2 : -0.55 eV

Smaller mixing for e_g

Larger mixing for t_{2g}

(2) Hirsh-Fye quantum monte carlo calculations

The magnetic behaviors of the Anderson impurity model at finite temperature are calculated by the Hirsh-Fye quantum Monte Carlo (QMC) technique.

Universal Kondo susceptibility for the one orbital case

ε_d = -U/2 (Symmetric case, constant DOS).

$$J_{sd} = \frac{2V^2U}{\varepsilon_d(\varepsilon_d + U)} = -\frac{8V^2}{U}$$

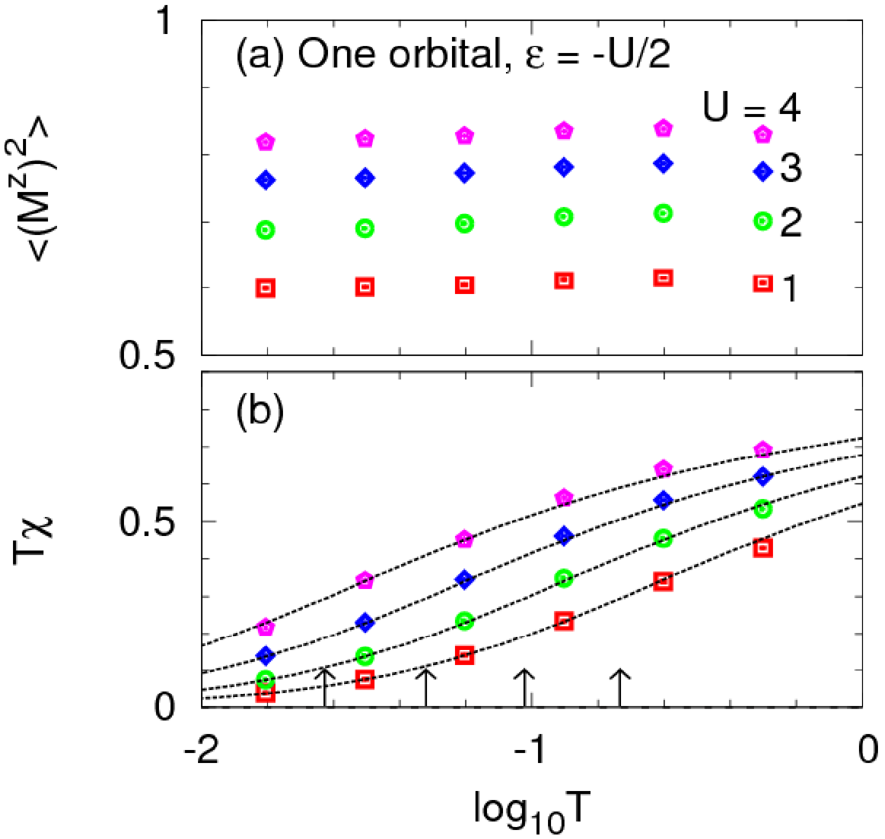

U = 1, 2, 3, 4 eV

T_K = 0.169, 0.0865, 0.0435, 0.0216 eV

1 eV ~ 10,000 K. 0.0216 eV ~ 200 K

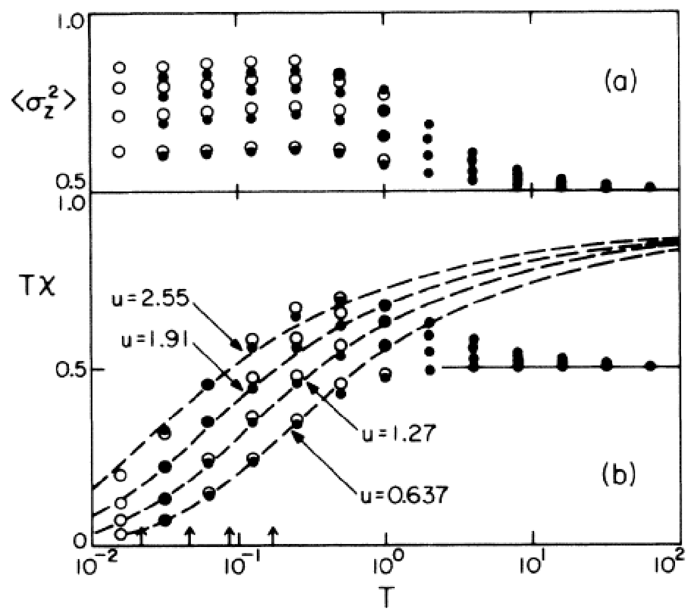

FIG. 2. (a) Local moment $\langle \sigma_z^2 \rangle$ and (b) $T\times$ (spin susceptibility) for a single Anderson impurity; $\Delta = 0.5$ and $u = 0.637$, 1.27, 1.91, and 2.55. The closed and open circles correspond to $\Delta\tau = 0.25$ and $\Delta\tau = 0.5$, respectively. The dashed lines are the universal Kondo susceptibility for the four values of T_K given in the text.

$u = U/\pi\Delta$

Hirsch and Fye, PRL 56, 2521(1986)

(3) Magnetic behaviors for Fe in Au (QMC results)

2-Orbitals case

$$\xi = 1 : z^2,$$

$$\xi = 2 : xz.$$

3-Orbitals case

$$\xi = 1 : z^2,$$

$$\xi = 2 : -\frac{1}{\sqrt{2}}(xz - iyz) : p_1 : l = 1, m = 1;$$

$$\xi = 3 : -\frac{1}{\sqrt{2}}(xz + iyz) : p_{-1} : l = 1, m = -1.$$

Local moment

$$M_\xi^z = n_{\xi\uparrow} - n_{\xi\downarrow},$$

Impurity magnetic susceptibility

$$\chi_\xi = \int_0^\beta d\tau \langle M_\xi^z(\tau) M_\xi^z(0) \rangle,$$

Occupation number

$$n_\xi = n_{\xi\uparrow} + n_{\xi\downarrow},$$

2-orbitals case, e_g and t_{2g}

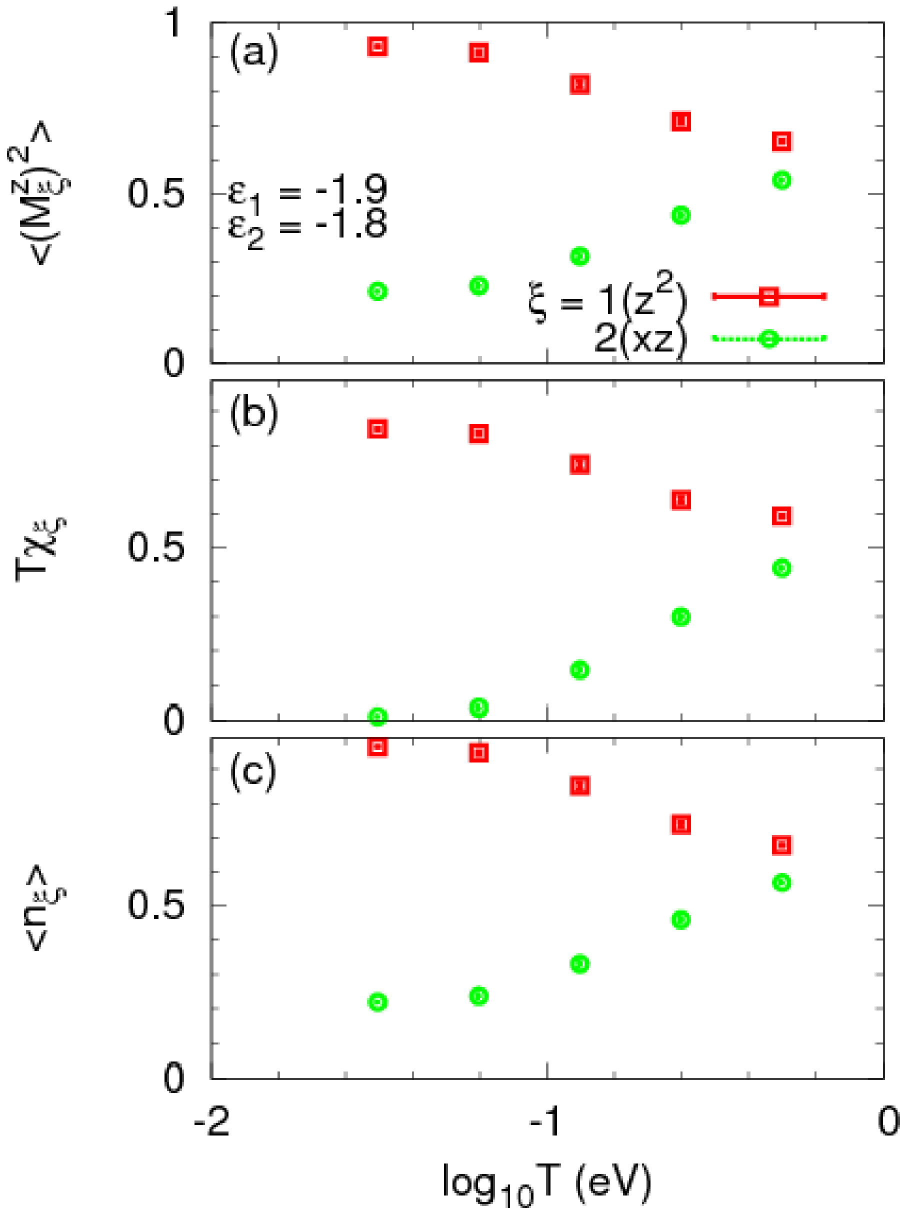

3-orbitals case, e_g and t_{2g}

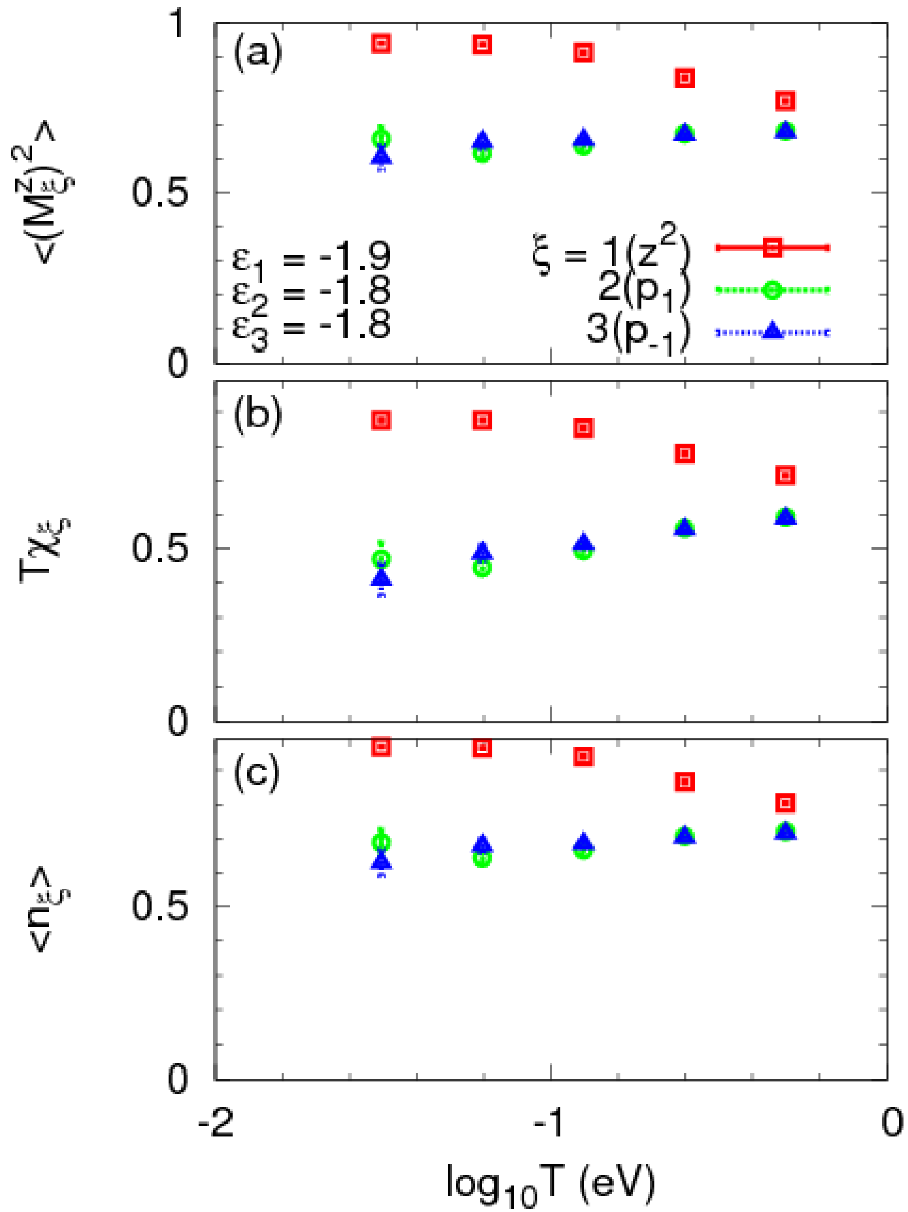

(4) Spin-orbit interaction within t_{2g} oribtals for Fe in Au

[Gu, et al., PRL105 (2009) 086401]

Ising-type spin-orbit interaction for *p*-electrons: $l=1$, $m=1,0,-1$.

$$H_{so} = (\lambda/2) \sum_{m,m',\sigma,\sigma'} d^{\dagger}_{m\sigma} (\mathbf{l})_{mm'} \cdot (\sigma)_{\sigma\sigma'} d_{m'\sigma'} ,$$

$$H_{so} = (\lambda/2) \sum_{m,\sigma} d^{\dagger}_{m\sigma} (\mathbf{l})^{z}_{mm} (\sigma)^{z}_{\sigma\sigma} d_{m\sigma} .$$

$$l^z = \begin{pmatrix} 1 & 0 & 0 \\ 0 & 0 & 0 \\ 0 & 0 & -1 \end{pmatrix}, \sigma^z = \begin{pmatrix} 1 & 0 \\ 0 & -1 \end{pmatrix},$$

$$H_{so} = (\lambda/2) \left(n_{1\uparrow} - n_{1\downarrow} - n_{-1\uparrow} + n_{-1\downarrow} \right) ,$$

T = 350 K, λ = 75 meV

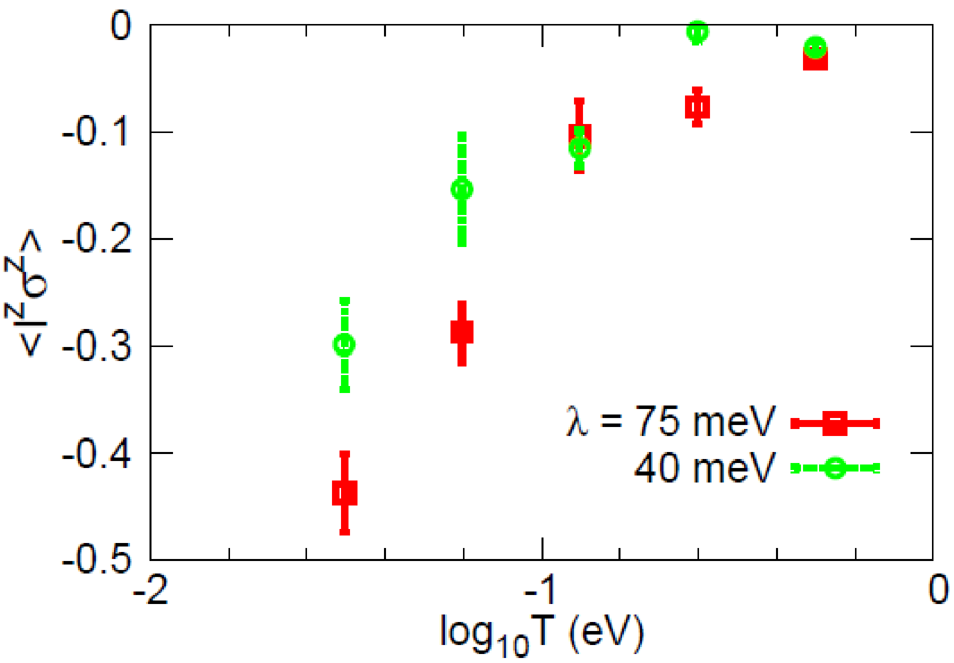

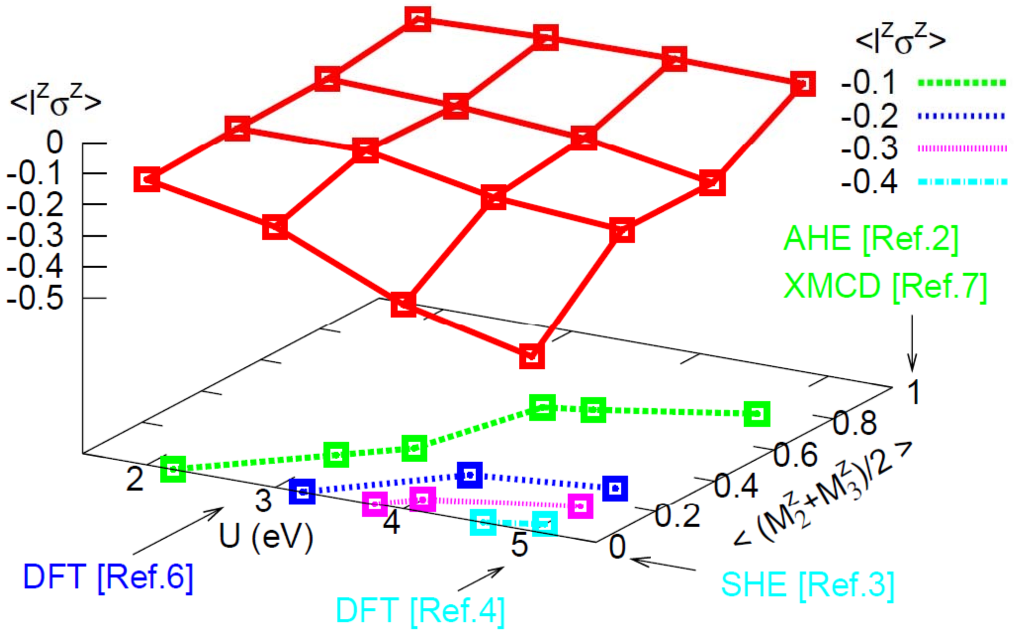

(5) Estimation of spin Hall angle for Fe impurity in Au

$$\gamma_s \cong -\frac{3\delta_1(\cos 2\delta_2^+ - \cos 2\delta_2^-)}{9\sin^2\delta_2^+ + 4\sin^2\delta_2^- + 3[1-\cos 2(\delta_2^+ - \delta_2^-)]}$$

Since we consider only two t_{2g} orbitals with $\ell_z = \pm 1$, the SOI within the t_{2g} orbitals gives rise to the difference in the occupation numbers between the parallel (n_P) and anti-parallel (n_{AP}) states of the spin and angular momenta. These occupation numbers are related to the phase shifts δ_P and δ_{AP}, through generalized Friedel sum rule, respectively, as $n_{P(AP)} = \delta_{P(AP)}/\pi$, and $\pi < \ell_z\sigma_z > = \delta_P - \delta_{AP}$, $\pi < n_2 > + \pi < n_3 > = \delta_P + \delta_{AP}$.

Putting $< \ell_z\sigma_z > = -0.44$ for $\lambda = 75$ meV, and $< n_2 > = < n_3 > = 0.65$, we obtain $\delta_P = 1.35$ and $\delta_{AP} = 2.73$.

Taking into account the estimate $\sin \delta_1 \sim= 0.1$, $\gamma_s \sim= 0.06$ is thus obtained.

[Seki, et al., Nat. Mater. 7 (2008)125]

$\gamma_s \sim= 0.11$ (exp.)

Influence of Fe Impurity on Spin Hall Effect in Au

Isamu Sugai[1], Seiji Mitani[2], and Koki Takanashi[1]

[1]Institute for Materials Research, Tohoku University, Sendai 980-8577, Japan
[2]National Institute for Materials Science, Tsukuba 305-0047, Japan

We investigated the influence of Fe impurity on spin Hall effect in Au using multi-terminal devices consisting of an FePt perpendicular spin polarizer and a Au Hall cross with different Fe impurity concentrations. As the Fe impurity concentration was increased in the range of 0–0.95 at.%, the resistivity of Au doped with Fe increased and the spin diffusion length decreased from 35 nm to 27 nm. On the other hand, the spin Hall angle for Au doped with Fe, evaluated from the spin injector-Hall cross distance dependence of spin Hall signals, was approximately 0.07, independent of the Fe concentration. The experimental results provide important information for understanding the mechanism of the large spin Hall effect.

Skew scattering
γ_s ~0.07 ,
independent of
Fe concentration.

PARAMETERS OF $P_{\underline{\mathrm{AuFe}}}$, $R_s^{\underline{\mathrm{AuFe}}}$, $\lambda_{\underline{\mathrm{AuFe}}}$, P AND α_H OBTAINED FOR THE PRESENT FePt/Au DEVICES

	$\rho_{\underline{\mathrm{AuFe}}}$ [μΩ·cm]	$\lambda_{\underline{\mathrm{AuFe}}}$ [nm]	$R_s^{\underline{\mathrm{AuFe}}}$ [Ω]	P	α_H
Non-doped Au	3.6	35 ± 4	1.1	0.038	0.07 ± 0.02
$Au_{99.58}Fe_{0.42}$	4.3	33 ± 3	1.3	0.034	0.07 ± 0.01
$Au_{99.05}Fe_{0.95}$	7.0	27 ± 3	1.7	0.027	0.07 ± 0.03

IV. Summary and Outlook

Summary

1. Spin Hall effect, a manifestation of special relativity, is rich of fundamental physics, and also related to such classic phenomena as Kondo effect.

2. Spin Hall effect may be used to generate, detect and even manipulate spin currents, and hence has important applications in such hot fields as spintronics.

3. *Ab initio* band theoretical calculations not only play an important role in revealing the mechanism of spin Hall effect, but also help in searching for new spintronic materials.

Outlook

1. Several fundamental problems remain to be addressed. For example, a general theory in terms of conserved spin current is still lacking. The question of spin Hall insulators and associated truely dissipationless spin current remain unanswered.

Spin Hall insulators (Fiction or fact?)

[Murakami, Nagaosa, Zhang, 2004 PRL93, 156804]

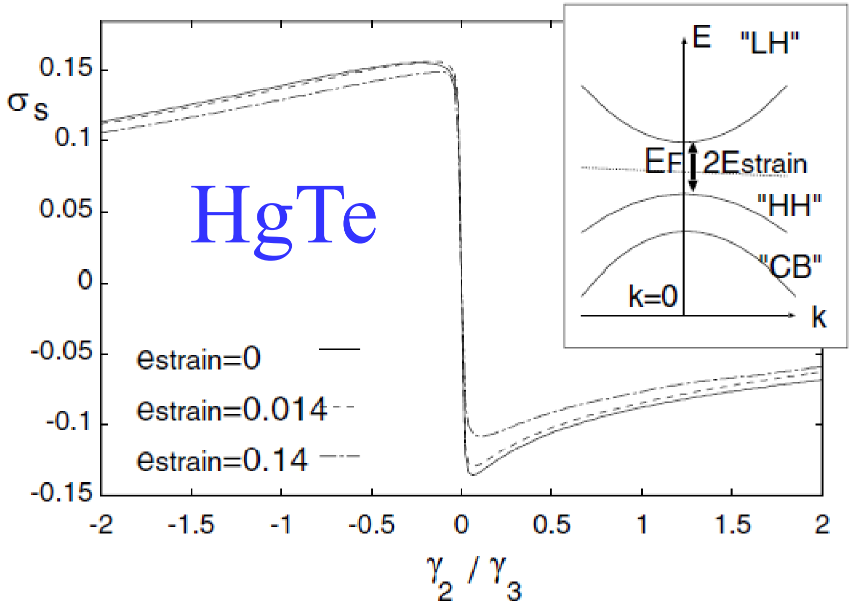

cubic NaCl structure

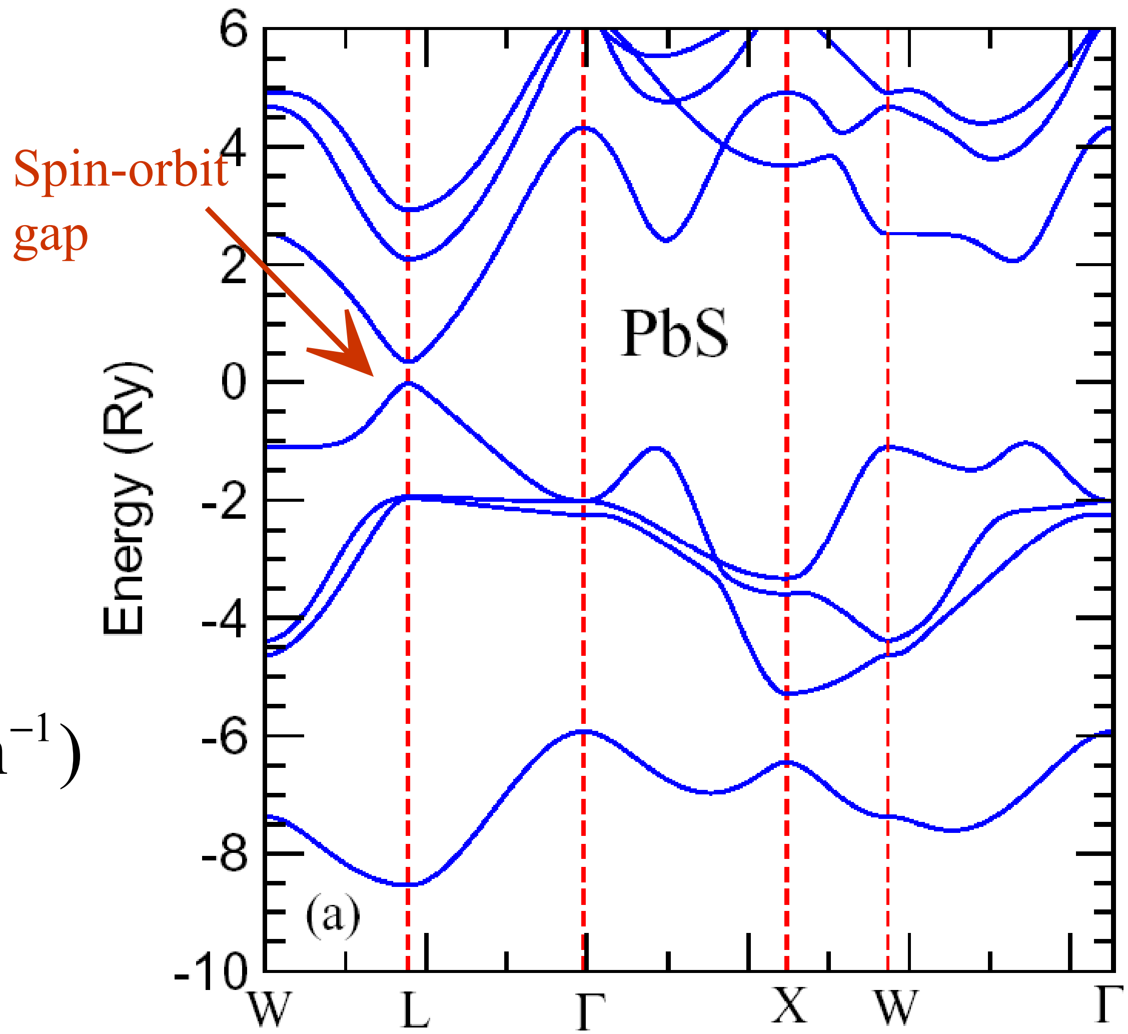

Undoped PbS

$$\sigma_{xy}^{s} = 57.5\ (\hbar/\mathrm{e})(\Omega^{-1}\mathrm{cm}^{-1})$$

[Guo, 2005, unpublished]

2. However, most activities in the field are currently focused on quantum spin Hall effect in topological insulators.

Zoo of the Hall Effects:

Ordinary Hall effect (Hall 1879);

Anomalous Hall effect (Hall 1880 & 1881);

Extrinsic spin Hall effect (Dyakonov & Perel 1971);

Integer quantum Hall effect (von Klitzing et al. 1980);

Fractional quantum Hall effect (Tsui et al. 1982);

Intrinsic spin Hall effect (Murakami et al. 2003; Sinova et al. 2004).

Quantum spin Hall effect (Kane & Mele 2005, Bernevig & Zhang 2006)

Topological insulators & quantum spin Hall effect

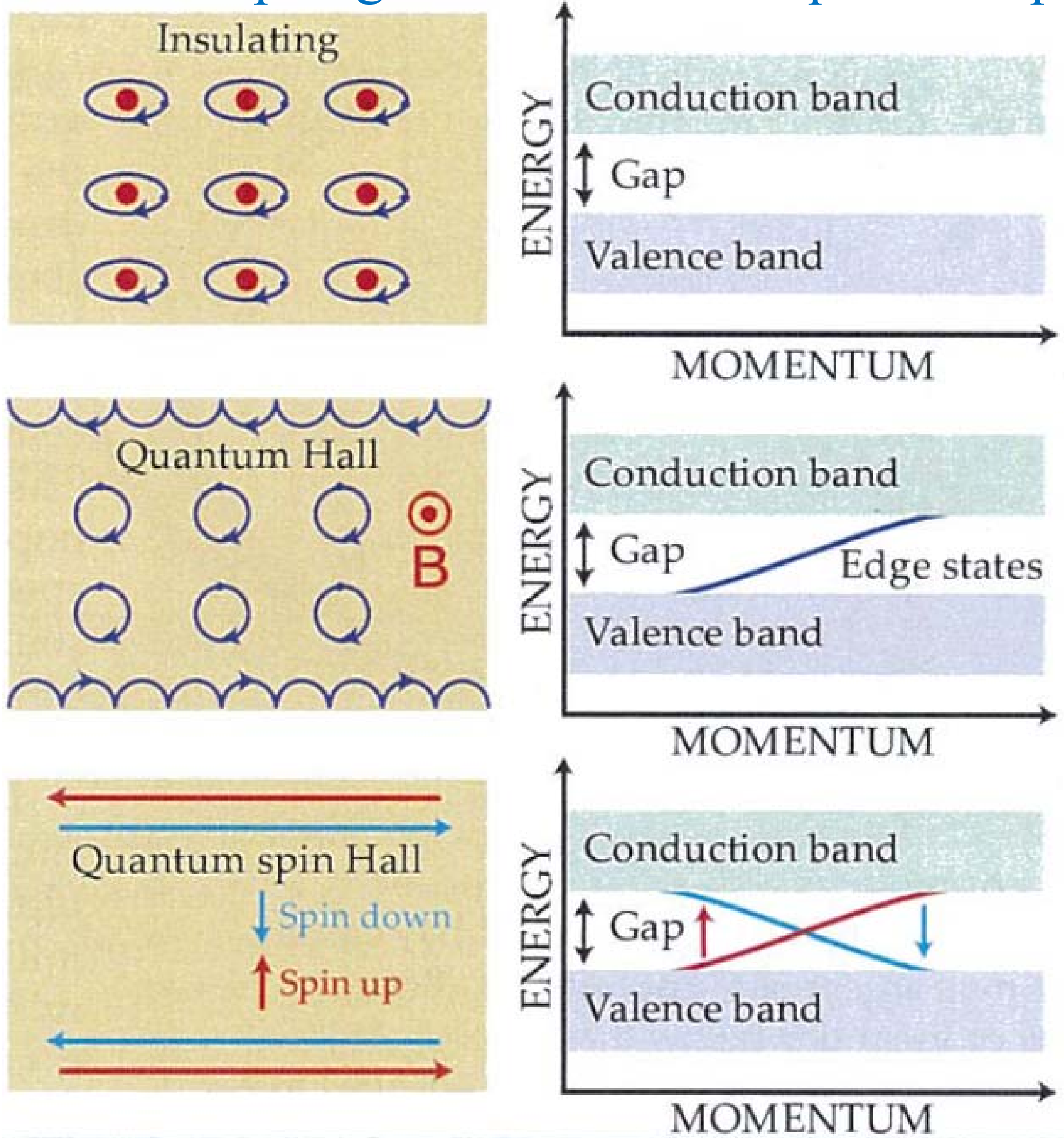

Ordinary insulators

Band gap, localization gap etc

Quantum Hall insulators

Gap due to Landau level formation induced by applied magnetic field

Topological invariant: Chern number

Topological insulators

Nonzero topological invariant Z_2:
Edge states: time reversal symmetry

[Day, PhysToday2008Jan 19]

(i) Zigzag graphene strips as 2D topological insulators

[Kane & Mele, PRL 2005]

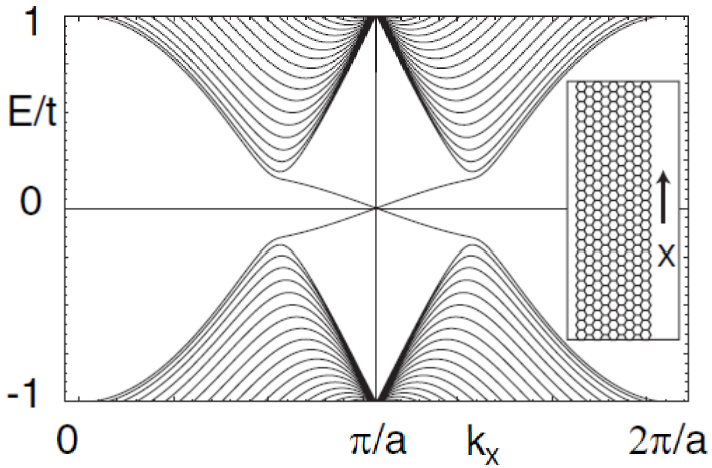

[Chen, Xiao, Guo 2010]

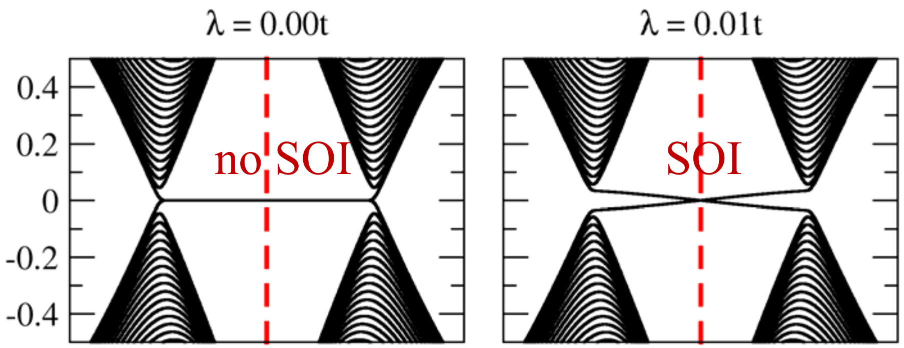

SOI is too small (<0.01 meV) to make QSHE observable!

(ii) Natural semiconductors as 3D topological insulators

[Bernevig Hughes, Zhang, Sci. 2006]

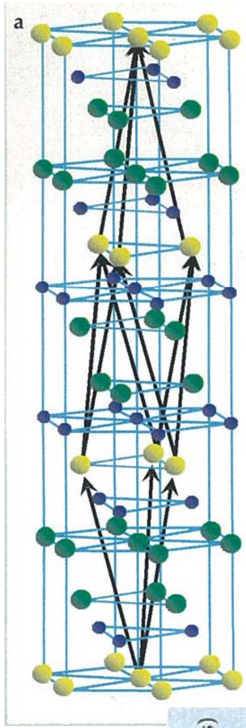

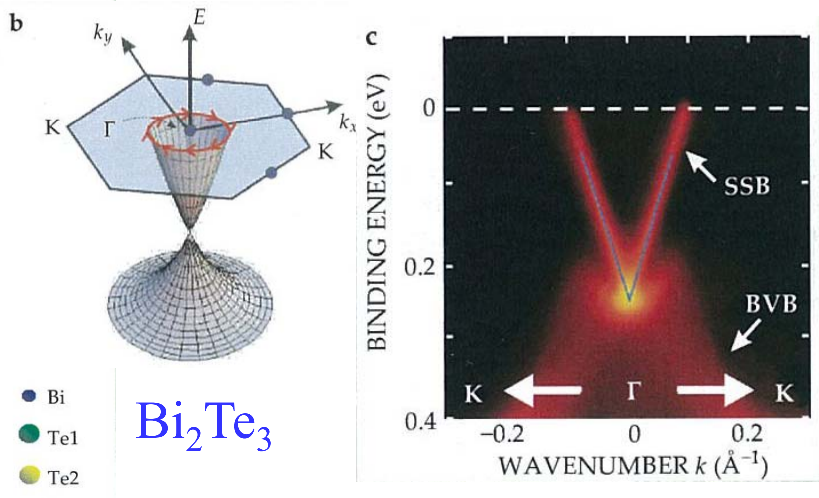

Bi_2Te_3

Chen et al. Science 2009]

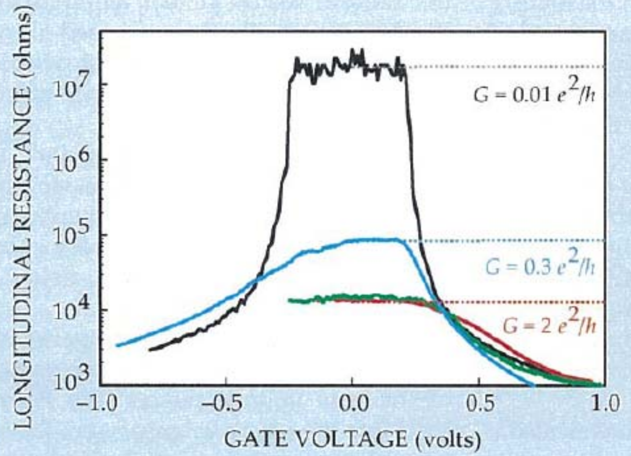

Figure 3. The quantum spin Hall effect features quantized edge currents. To be sure of seeing them, the Würzburg group gated their device to sweep the Fermi level from the valence band, through the bandgap, and into the conduction band. The black trace comes from a sample whose thickness (d < 6.3 nm) ensures that it behaves like a normal insulator. When the Fermi level lies in the bandgap, resistance is high. The red, green, and blue traces come from samples whose thickness (d > 6.3 nm) ensures that they can carry edge states. Quantization of the conductance G is observed when the sample is shorter than the electrons' mean free path. That's the case for the red and green traces but not for the blue trace. (Adapted from ref. 5.)

[Koenig et al. Sci 2007]

Acknowledgements:

Discussions and Collaborations:

Qian Niu (UT Austin), Yugui Yao (IOP, CAS)

Tsung-Wei Chen & Hsiu-Chuan Hsu (Nat'l Taiwan U.)

Yang-Fang Chen and his exp. team (Nat'l Taiwan U.)

Naoto Nagaosa (Tokyo U.)

Shuichi Murakami (Tokyo Inst. Techno.)

Bo Gu, Sadamichi Maekawa (Tohoku U.)

Refs: [on *p*-type zincblende semiconductors, PRL 94, 226601 (2005)]
[on Rashba & Dresselhaus models, PRB73 (2006) 235309]
[on *n*-type wurtzite nitride semiconductors, PRL 98, 136403 (2007)]
[on ISHE in platinum metal, PRL 100, 096401 (2008)]
[on ESHE & Kondo effect in Fe in Au, PRL 102, 036401 (2009)]
[on QMC of Kondo effect in Fe in Au, PRL 105, 086401 (2010)]

Financial Support:

National Science Council of Taiwan.